WILEY

# Reaction wheel pendulum control using fourth-order discontinuous integral algorithm

**Diego Gutiérrez-Oribio**[1] | **Ángel Mercado-Uribe**[2] | **Jaime A. Moreno**[2] | **Leonid Fridman**[1]

[1]Departamento de Control y Robótica, División de Ingeniería Eléctrica, Facultad de Ingeniería, Universidad Nacional Autónoma de México (UNAM), Ciudad de México, Mexico

[2]Eléctrica y Computación, Instituto de Ingeniería, Universidad Nacional Autónoma de México (UNAM), Ciudad de México, Mexico

**Correspondence**
Leonid Fridman, Departamento de Control y Robótica, División de Ingeniería Eléctrica, Facultad de Ingeniería, Universidad Nacional Autónoma de México (UNAM), 04510 Ciudad de México, Mexico.
Email: lfridman@unam.mx

**Funding information**
Consejo Nacional de Ciencia y Tecnología, Grant/Award Number: 282013, CVU: 624679, CVU: 705765; Programa de Apoyo a Proyectos de Investigación e Innovación Tecnológica, Grant/Award Number: IN115419, IN110719

**Summary**
The fourth-order model of the reaction wheel pendulum is considered and a fourth-order discontinuous integral algorithm is used for stabilization and tracking of the system, using a continuous control signal. The states reach the origin or a reference signal in finite-time, even in presence of uncertain control coefficient and a kind of matched and unmatched uncertainties/disturbances. A homogeneous Lyapunov function is designed to ensure local finite-time stability of the system, which can be used for designing the controller gains. Simulations and experimental results illustrate the performance and advantages of the presented algorithm.

**KEYWORDS**
finite-time convergence, higher-order sliding-mode control, nonlinear control, tracking control, wheel pendulum

## 1 | INTRODUCTION

The reaction wheel pendulum (RWP) is a simple underactuated mechanical system that posses important and challenging control issues, so that it has become the object of many research publications. The local stabilization task, that is, to drive the states to the upright position of the pendulum (the origin of the system) when the pendulum is close to it, is one of the topics most studied for this system. This task has been solved using different control techniques, for example, state-feedback linearization,[1] sliding-modes[2-4] or passivity-based control with interconnection and damping assignment.[5,6]

Although the RWP is a two-degrees-of-freedom system, and it has therefore four state variables, many authors consider the stabilization problem without paying attention to the wheel position, and thus reducing the model to just three states. This reduced-order model can be transformed to the controllability normal form, that is, a third-order linear chain of integrators, by using a state diffeomorphism plus a state feedback (see, eg, References 1,3, and 7). However, this approach is only valid *locally*, since there is a singularity when the pendulum position is horizontal.

**Abbreviations:** 3-DIA, third order discontinuous integral algorithm; 4-DIA, fourth order discontinuous integral algorithm; RWP, reaction wheel pendulum.

An important aspect not properly considered in the previous works is the presence of uncertainties in the model, for example, parameters, and external perturbations acting on the system. Dealing appropriately with this requires the use of robust control schemes, for example, the classical or higher order sliding-mode techniques,[8] which are able to compensate (theoretically) exactly bounded and matched persistent uncertainties and/or disturbances. In chapter 6 in Reference 9 and Reference 10 for example, the perturbed model of the RWP system is used to solve the tracking problem of the pendulum dynamics, using a sliding-mode algorithm. However, this is at the cost of having a discontinuous control signal, with the consequent undesirable chattering effect.

A different alternative to deal with matched disturbances, is the addition of an integral action (see, eg, Reference 11), which is used in the classical control theory to cope with constant perturbations. One way to join higher-order sliding-mode and integral control is provided by the so-called continuous higher-order sliding-mode (CHOSM) controllers (see References 12-16). These algorithms consist of a continuous static homogeneous finite-time state-feedback controller for the nominal model of the system, aimed at stabilizing the closed-loop, and a discontinuous integral action to compensate for the uncertainties/perturbations. The resulting homogeneous sliding-mode controllers produce a continuous control signal and they are able to compensate theoretically exactly Lipschitz perturbations, that is, signals with a bounded derivative, which are nonvanishing, that is, they are not zero at the equilibrium point. Moreover, the effect of chattering caused by the discontinuity and discretization is strongly attenuated. It is shown in Reference 17, that CHOSM controllers, in the presence of sufficiently fast actuators and small-time delay, generate oscillations with a smaller amplitude and consume less energy to maintain the system in a practical sliding-mode than sliding-mode algorithms with discontinuous control signal. The first CHOSM algorithm, used for systems with relative degree one, was the super-twisting.[18,19] It was followed by some others like the continuous twisting[15,20] and the discontinuous integral algorithms,[14,16,21] for higher relative degrees.

In a previous work of the authors[4], a third-order model of the RWP was used for the local stabilization of the origin (upward position), considering matched Lipschitz disturbances/perturbations under the assumption that the control coefficient was known. For this task, a third-order discontinuous integral algorithm (3-DIA) was developed, based on a locally valid state transformation.

The objective of this article is to solve the robust and local *stabilization* problem and the *tracking* of a rather arbitrary reference signal for the *the fourth-order* model of the RWP, considering Lipschitz matched uncertainties/perturbations and an *uncertain control* coefficient. We use a *global* state transformation to design a fourth-order discontinuous integral algorithm (4-DIA) to fully solve both problems. The proposed algorithm ensures the finite-time convergence to a fifth-order sliding-mode, which attains a better precision than the 3-DIA developed previously in Reference 4. We provide the gains for the 4-DIA and evaluate its performance by means of a simulation study and experimental validation on a laboratory set-up. Further, we compare its behaviour and precision with the 3-DIA.

This article is organized as follows. The system model is presented in Section 2 and the problem statement is given in Section 3. The 4-DIA, gain scaling, and tracking design are presented in Section 4, describing the main results of this article. Section 5 contains the simulation study and the experimental validation. A comparative precision analysis between the 3-DIA and the 4-DIA is presented in Section 6. Finally, some concluding remarks are given in Sections 8 and 7. Some preliminary results and the proof of the Theorems are presented in the Appendices.

*Notation:* The signed power function, defined by $\lceil \cdot \rfloor^\gamma := | \cdot |^\gamma \text{sign}(\cdot)$, for any $\gamma \in \mathbb{R}_{\geq 0}$, will be used throughout the work.

## 2 | RWP MODEL

The RWP, which is illustrated in Figure 1, consists of a pendulum rotating in a vertical plane, with its pivot pin fixed to a stationary base, and a rotating wheel attached to the pendulum at the other extreme. The rotary axes of the pendulum and the wheel are parallel to each other. The wheel is actuated by a motor, producing a torque $\tau$ [Nm]. The four states describing the RWP are $x = [x_1, x_2, x_3, x_4]^T$, where $x_1$ [rad] is the angle between the upward direction and the pendulum. $x_1 = 0$ for the upright position of the pendulum and it increases in the counter-clockwise direction. $x_2$ [rad/sec] is the angular velocity of the pendulum, $x_3$ [rad] is the angular position of the wheel, and $x_4$ [rad/sec] is its angular velocity.

**FIGURE 1** Reaction wheel pendulum system [Colour figure can be viewed at wileyonlinelibrary.com]
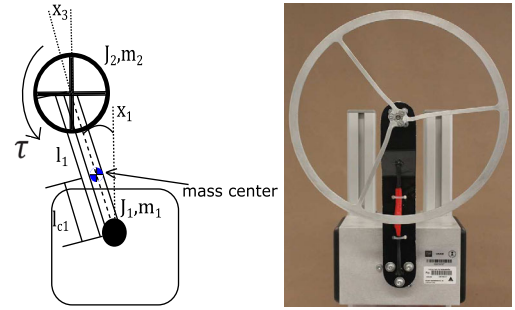


The system dynamics was presented in Reference 22 and is described by the following equations:

$$\dot{x}_1 = x_2,$$
$$\dot{x}_2 = \frac{d_{22}W\sin(x_1) + d_{12}b_2x_4 - d_{12}\tau}{D},$$
$$\dot{x}_3 = x_4,$$
$$\dot{x}_4 = \frac{-d_{21}W\sin(x_1) - d_{11}b_2x_4 + d_{11}\tau}{D}, \tag{1}$$

where

$$d_{21} = d_{12} = d_{22} = J_2,$$
$$d_{11} := m_1l_{c1}^2 + m_2l_1^2 + J_1 + J_2,$$
$$D := d_{11}d_{22} - d_{12}d_{21} > 0,$$
$$\overline{m} := m_1l_{c1} + m_2l_1, \quad W = \overline{m}g.$$

$m_1$ is the mass, $J_1$ is the momentum of inertia, $l_1$ is the length of the pendulum, while $l_{c1}$ is the position of its center of mass. $m_2$ is the mass and $J_2$ is the momentum of inertia of the wheel. $\overline{m}$ represents the equivalent mass of the system, $d_{11}$ is the equivalent momentum of inertia of the system, $b_2$ is the friction coefficient of the wheel, and $g$ is acceleration of the gravity.

The previous model, excluding the position of the wheel $x_3$, is transformed in Reference 1 to the third-order (normal) controller form. However, this transformation has a singularity when the pendulum is in the horizontal position, so that the resulting normal form is only valid locally. In this article we choose to use a *global diffeomorphism* to transform the *full-order* model (1) into a form *close* to the fourth-order controller form, which is valid globally. Specifically, we use the linear diffeomorphism

$$z_1 = d_{11}x_1 + d_{12}x_3,$$
$$z_2 = d_{11}x_2 + d_{12}x_4,$$
$$z_3 = x_1,$$
$$z_4 = x_2, \tag{2}$$

to bring the system (1) to the form

$$\dot{z}_1 = z_2,$$
$$\dot{z}_2 = W\sin(z_3),$$
$$\dot{z}_3 = z_4,$$
$$\dot{z}_4 = \frac{d_{22}W\sin(z_3) + b_2(z_2 - d_{11}z_4) - d_{12}\tau}{D}. \tag{3}$$

Applying the (linearizing) state-feedback

$$\tau_{nom} = \frac{d_{22}W\sin(z_3) + b_2(z_2 - d_{11}z_4) - Dv}{d_{12}}, \tag{4}$$

we arrive to the system

$$\dot{z}_1 = z_2 \ ,$$
$$\dot{z}_2 = W \sin(z_3) \ ,$$
$$\dot{z}_3 = z_4 \ ,$$
$$\dot{z}_4 = v \ . \tag{5}$$

System (5) is *globally* feedback-equivalent to (1), it has a form *close* to the controller normal form, since its output $z_1$ has relative degree 4 with respect to the new control input $v$, and it is a chain of integrators, except for the term $\phi(z_3) \triangleq W \sin(z_3)$. Note that this nonlinear term $\phi(z_3)$ is locally, near $z_3 = 0$, linear, that is, $\phi(z_3) \approx W z_3$, so that (5) has a linearization which is (basically) the controller normal form. Note that $\phi(z_3)$ restricts the action of the "virtual" control variable $z_3$ on the subsystem $(z_1, z_2)$ as a kind of saturation. However, in this article, we will use the form (5) to design a *local* (near $x = 0$) control law, so that the nonlinear effect of $\phi(z_3)$ does not need to be considered, but in contrast to the previous works we will have a global description of the closed-loop system.

## 3 | PROBLEM STATEMENT

Our objective is to force the output $y = z_1$ to track a time-varying signal $r(t)$ in finite-time, that is, for every $t \geq T$, the output $y(t) = z_1(t) \equiv r(t)$ for some $T > 0$. We will require this not for an arbitrary initial condition, but for initial conditions close to the upward position of the pendulum, that is, $z = 0$, so we want to attain a *local* tracking controller. Furthermore, we require of $r(t)$ to have continuous and bounded derivatives up to order four, and to have a fifth time derivative almost everywhere which is bounded, that is, $r^{(i)}(t)$ exist and are continuous for $i = 1, \ldots, 4$ and it exists almost everywhere and it is bounded where it exists for $i = 5$. Moreover, since the controller solves the problem *locally* we require the reference and its derivatives also not only to be bounded but also to be sufficiently *small*, such that the attraction region of the controller is not abandoned. When the reference is identically zero, that is, $r(t) \equiv 0$, then the tracking problem becomes a (local) *stabilization* problem for the equilibrium $z = 0$ at the upward position of the RWP. So we treat both problems in a unified manner.

We consider (bounded) reference signals that are generated by the system

$$r_1(t) = r(t) \ , \quad \dot{r}_1(t) = r_2(t) \ , \quad \dot{r}_2(t) = W \sin(r_3(t)) \ , \quad \dot{r}_3(t) = r_4(t) \ , \quad \dot{r}_4(t) = r_5(t) \ , \quad \dot{r}_5(t) \in R[-1 \ , +1] \ ,$$

where $[-1 \ , +1] \in \mathbb{R}$ is the closed interval bounded by $-1$ and $+1$. This differential inclusion for the reference represents a signal that can be tracked by the system, with a bounded derivative $\dot{r}_5(t)$. The tracking errors for the states $z$ are naturally defined as

$$e_1 = z_1 - r_1 \ ,$$
$$e_2 = z_2 - r_2 \ ,$$
$$e_3 = z_3 - r_3 \ ,$$
$$e_4 = z_4 - r_4 \ , \tag{6}$$

and the tracking error dynamics for the nominal system (5) is given by

$$\dot{e}_1 = e_2,$$
$$\dot{e}_2 = W(\sin(e_3 + r_3) - \sin(r_3)),$$
$$\dot{e}_3 = e_4,$$
$$\dot{e}_4 = v - r_5(t) \ . \tag{7}$$

Since the transformed model (5) has been obtained under the assumption that the parameters of the system are perfectly known, the tracking error dynamics (7) is also only valid in the nominal case of perfectly known model parameters. If this is not the case, the application of the (linearizing) state-feedback (4) with uncertain parameters will not lead to system (5). In particular, if we assume that the values we know for the parameters is represented by a superindex "s" (the

"supposed" values of the parameters), the actually applied feedback (4) will have the form

$$\tau = \frac{d_{22}^s W^s \sin(z_3) + b_2^s(z_2 - d_{11}^s z_4) - D^s \nu}{d_{12}^s} \, , \tag{8}$$

and, assuming that we can measure (or estimate) the states $e_i$, we arrive to the more realistic tracking error dynamics

$$\begin{aligned}
\dot{e}_1 &= e_2, \\
\dot{e}_2 &= We_3 + W\psi(t, e_3) \, , \\
\dot{e}_3 &= e_4, \\
\dot{e}_4 &= \beta(t, e)[\nu + \varphi_1(t, e) + \varphi_2(t, e)] \, ,
\end{aligned} \tag{9}$$

where

$$\begin{aligned}
\beta(t, e) &= \frac{D^s d_{12}}{D d_{12}^s} \, , \\
\psi(t, e_3) &= \sin(e_3 + r_3) - \sin(r_3) - e_3 \, , \\
\varphi_1(t, e) &= \delta_1[\sin(e_3 + r_3) - \sin(r_3)] - \delta_3 e_4 \, , \\
\varphi_2(t, e) &= \delta_2 e_2 + \delta_1 \sin(r_3(t)) + \delta_2 r_2(t) - \delta_3 r_4(t) - \delta_4 r_5(t) \, .
\end{aligned} \tag{10}$$

The parameters $\delta_i$ are given by

$$\delta_1 = \left( \frac{d_{12}^s d_{22} W}{D^s d_{12}} - \frac{d_{22}^s W^s}{D^s} \right) \, , \quad \delta_2 = \left( \frac{d_{12}^s b_2}{D^s d_{12}} - \frac{b_2^s}{D^s} \right) \, , \quad \delta_3 = \left( \frac{d_{12}^s b_2 d_{11}}{D^s d_{12}} - \frac{b_2^s d_{11}^s}{D^s} \right) \, , \quad \delta_4 = \frac{D d_{12}^s}{D^s d_{12}} \, ,$$

and they result from the uncertainty in the values of the true parameters. Note that $\delta_1 = \delta_2 = \delta_3 = 0$ and $\delta_4 = 1$ when there is no parameter uncertainty.

Function $\psi(t, e_3)$, which is for our local analysis a perturbation of the linear function $e_3$, is vanishing at zero, that is, $\psi(t, 0) = 0$, and so is also the uncertain term $\varphi_1(t, e)$, since $\varphi_1(t, 0) = 0$. However, the perturbation term $\varphi_2(t, e)$ is not vanishing at zero, that is, $\varphi_2(t, 0) \neq 0$. Note that, even if we know the reference signals $r_i(t)$, $\varphi_2(t, e)$ cannot be compensated (with a memoryless continuous control feedback) due to our lack of knowledge of the values of the parameters $\delta_i$.

Model (9) is more suitable to design a controller taking into account effects occurring in a real situation. So our objective is to solve the local, robust and finite-time tracking (and stabilization) problem for the RWP. For model (9), this is equivalent to the robust stabilization of the origin $e = 0$. We will assume that the control coefficient $\beta$, the vanishing perturbation/uncertain terms $\psi$ and $\varphi_1$, and the nonvanishing perturbation term $\varphi_2$ satisfy the following conditions, for some positive constants $L_0, b_m, b_M, L_1,$ and $L$:

$$\begin{aligned}
|\psi(t, e_3)| &\leq L_0 |e_3| \, , \quad 0 < b_m \leq \beta(t, e) \leq b_M \, , \\
|\varphi_1(t, e)| &\leq L_1 \left( |e_1|^{\frac{1}{5}} + |e_2|^{\frac{1}{4}} + |e_3|^{\frac{1}{3}} + |e_4|^{\frac{1}{2}} \right) \, , \quad |\dot{\varphi}_2(t, e)| \leq L \, .
\end{aligned} \tag{11}$$

The latter condition on the nonvanishing perturbation $\varphi_2$ requires it to have a bounded derivative (where it exists), that is, it is a Lipschitz function of time. These conditions (11) are clearly satisfied (at least locally) for the situation considered in (10). In the generalized form (11) further uncertain and/or perturbation effects can be considered.

## 4 | MAIN RESULT: THE DISCONTINUOUS INTEGRAL CONTROLLER

Since the non-vanishing perturbations cannot be fully compensated by means of a continuous state-feedback, and in order to attenuate the chattering effect, we will use the Following Fourth-Order Discontinuous Integral Sliding-Mode Algorithm (4-DIA) to solve these problems (see, eg, Reference 16):

$$\begin{aligned}
\nu &= -\lambda^{\frac{1}{2}} k_4 \left[ \lambda^{\frac{3}{2}} \kappa_1 e_1 + \lambda^{\frac{5}{4}} \kappa_2 \lceil e_2 \rfloor^{\frac{5}{4}} + \lambda^{\frac{5}{6}} \kappa_3 \lceil e_3 \rfloor^{\frac{5}{3}} + \lceil e_4 \rfloor^{\frac{5}{2}} \right]^{\frac{1}{5}} + \zeta, \\
\dot{\zeta} &= -\lambda k_{I1} \left[ e_1 + \lambda^{-\frac{1}{4}} k_{I2} \lceil e_2 \rfloor^{\frac{5}{4}} + \lambda^{-\frac{2}{3}} k_{I3} \lceil e_3 \rfloor^{\frac{5}{3}} + \lambda^{-\frac{3}{2}} k_{I4} \lceil e_4 \rfloor^{\frac{5}{2}} \right]^0 \, , \quad \lambda > 0 \, . \tag{12}
\end{aligned}$$

These controllers consist of two terms: (i) a homogeneous and continuous state-feedback, which is able to stabilize in finite-time the origin of the closed-loop system (without integral term) in the absence of nonvanishing perturbations. (ii) The integral term, which is a homogeneous and *discontinuous* function and is able to *estimate* in finite-time, and *fully compensate* for the persistent perturbations, if they have a bounded derivative, that is, are Lipschitz. Note that this is a surprising property for an integral control action, since, for example, classical PI controllers are only able to compensate for *constant* nonvanishing perturbations. Note also that the control signal $v(t)$ is *continuous*, despite of the discontinuity in the integral controller. This is the case, since the discontinuous signal at the output of the *sign* function $\lceil x \rfloor^0$ is integrated and then added to the feedback control signal to obtain $v$.

The closed-loop composed of the (transformed) tracking error dynamics for the RWP (9) and the 4-DIA controller (12) is given by

$$
\begin{aligned}
\dot{e}_1 &= e_2, \\
\dot{e}_2 &= We_3 + W\psi(t,\ e_3), \\
\dot{e}_3 &= e_4, \\
\dot{e}_4 &= \beta(t,\ e)\left[ -\lambda^{\frac{1}{2}}k_4\left[ \lambda^{\frac{3}{2}}\kappa_1 e_1 + \lambda^{\frac{5}{4}}\kappa_2\lceil e_2 \rfloor^{\frac{5}{4}} + \lambda^{\frac{5}{6}}\kappa_3\lceil e_3 \rfloor^{\frac{5}{3}} + \lceil e_4 \rfloor^{\frac{5}{2}} \right]^{\frac{1}{5}} + \zeta + \varphi_1(t,\ e) + \varphi_2(t,\ e) \right], \\
\dot{\zeta} &= -\lambda k_{I1}\left[ e_1 + \lambda^{-\frac{1}{4}}k_{I2}\lceil e_2 \rfloor^{\frac{5}{4}} + \lambda^{-\frac{2}{3}}k_{I3}\lceil e_3 \rfloor^{\frac{5}{3}} + \lambda^{-\frac{3}{2}}k_{I4}\lceil e_4 \rfloor^{\frac{5}{2}} \right]^0.
\end{aligned}
\tag{13}
$$

The following theorem presents the main result of the article, establishing the *local* finite-time stability result for system (13), and in turn for the 4-DIA applied to the RWP system described by (1). Note that in this latter case the control variable $\tau$ takes the form (8), where $v$ is given by the 4-DIA (12).

**Theorem 1.** *Suppose that the reference signal $r(t)$ satisfies the stated conditions. Consider the error tracking dynamics given by (9) and assume that the uncertain control coefficient $\beta(t,\ e)$, the vanishing uncertainty/perturbation $\varphi_1(t,\ e)$, the nonvanishing perturbation $\varphi_2(t,\ e)$ and the term $\psi_1(t,\ e_3)$ satisfy the conditions (11) with arbitrary positive constants $b_m$, $b_M$, $L_1$ and $L$, and a sufficiently small $L_0$. Select the integral gains $k_{I2}$, $k_{I3}$, $k_{I4}$ as arbitrary real numbers (including zero). Under these conditions, there exist positive gains $\kappa_1$, $\kappa_2$, $\kappa_3$, $k_4$ and $k_{I1}$, and a positive value $\lambda^*$ such that the point $e = (e_1,\ e_2,\ e_3,\ e_4) = 0$ is locally finite-time stable for system (13) for any value of $\lambda \geq \lambda^*$. Moreover, the integral variable $\zeta$ converges in finite-time to the nonvanishing perturbation signal $-\varphi_2(t, e)$.* □

The proof of this Theorem is presented in Appendix B, using a Lyapunov-based analysis.

Note that it is possible to obtain fitting gains for arbitrary values of the Lipschitz constant $L$ of the matched nonvanishing perturbation $\varphi_2$, any growth gain $L_1$ of the unmatched vanishing perturbation $\varphi_1$ and any bounds $0 < b_m \leq b_M$ of the uncertain control coefficient. Naturally, since the stabilization result is only local, these parameters cannot have arbitrarily large values.

The local character of the stability (proof) is a consequence of the nonlinearity $\psi(t,\ e_3)$, that appears due to the dynamical relation $\dot{z}_2 = W \sin(z_3)$ in the system. Since the sinus function is bounded and periodic, the effect of $z_3$ on $z_2$ is "saturated" and non monotonic. The saturation has as result that the value of $z_2$ cannot be changed as fast as desired or required, and a linear or homogeneous (virtual) control law cannot deal correctly with this situation. The non monotonic character of sinus makes also difficult for a homogeneous controller to behave suitably. Our results, which rely strongly on homogeneity, are not adapted to the global situation, but they perform very well locally.

The functioning of the proposed integral controller to fully counteract the time-varying perturbation $\varphi_2$ can be understood from the fact that the integral variable $\zeta$ converges in finite time to the perturbation, that is, $\zeta(t) = -\varphi_2(t,\ e)$ after some time $t \geq T$. This means that the integral control estimates exactly and in finite time the perturbation, so that it can compensate for it in closed-loop. This is very much the same what happens with the integral action in the classical PI control. However, for the DIA this works out for *time-varying* perturbations, while for the PI control it succeeds only for *constant* ones.

## Gain design and tuning

Appropriate gains for the 4-DIA algorithm are derived using a strong and smooth Lyapunov function in Appendix B. In particular, in Sections B.2.2 and B.3, the calculation procedure is derived for the gains without and with the perturbation

**TABLE 1** Some calculated set of gains for the 4-DIA

| Set | $k_1$ | $k_2$ | $k_3$ | $b_m k_4$ |
|---|---|---|---|---|
| 1 | 2 | 2 | 5 | 45 |
| 2 | 2 | 2 | 20 | 55 |
| 3 | 2 | 3 | 7 | 45 |

term $\varphi_1$, respectively. For the details we refer the reader to those subsections. Specific values of the gains are obtained by maximizing some homogeneous functions of degree zero, which are derived from the Lyapunov function. These maximizations are usually performed in a numerical way. In the following paragraphs, we present the main results, and the main steps to use a given set of stabilizing gains.

In order to design the gains of the 4-DIA, the following procedure is to be used:

1. First, the gains $k_1$, $k_2$ and $k_3$ are obtained.
   (a) Choose any positive value for $k_1 > 0$. Calculate the value $\mathcal{K}_2(k_1)$, depending on $k_1$, given by (B8).
   (b) Choose a gain $k_2 > \mathcal{K}_2(k_1)$. Calculate the value $\mathcal{K}_3(k_1, \ k_2)$, depending on $k_1, k_2$, given by (B8).
   (c) Choose a gain $k_3 > \mathcal{K}_3(k_1, \ k_2)$.
2. Select arbitrary values for the gains $k_{I2}$, $k_{I3}$, and $k_{I4}$, including zero. Choose a value $0 \le \overline{L} < 1$. Calculate the value $\mathcal{K}_{I1}(k_1, \ k_2, \ k_3, \ k_{I2}, \ k_{I3}, \ k_{I4}, \overline{L})$, given by (B8).
3. Choose a value $\frac{1}{\tilde{k}_{I1}} > \mathcal{K}_{I1}(k_1, \ k_2, \ k_3, \ k_{I2}, \ k_{I3}, \ k_{I4}, \ \overline{L})$. Set the value of $L_1$. Calculate the value $\mathcal{K}_{4, \ p}(k_1, \ k_2, \ k_3, \ k_{I2}, \ k_{I3}, \ k_{I4}, \ \overline{L}, \ \tilde{k}_{I1}, \ b_M L_1)$, given by (B9).
4. Given the value of $b_m$ choose the gain $k_4 > \frac{1}{b_m} \mathcal{K}_{4, \ p}$.
5. Calculate $k_{I1} = k_4 \tilde{k}_{I1}$, $L^* = \overline{L} k_{I1}$ and $\lambda^* = \frac{L}{L^*}$. Choose $\lambda \ge \lambda^*$.

Note that the gains $k_1$, $k_2$, and $k_3$ do not depend on any others. For fixed values of $\overline{L}$ and the gains $k_{I2}$, $k_{I3}$ and $k_{I4}$, one can calculate $\tilde{k}_{I1}$. Fixing also a value of $b_M L_1$, it is also possible to obtain a value of $k_4$. Alternatively to the last items in the previous procedure, it is possible to use these values of the gains and just increase the value of the scaling parameter $\lambda$ to attain stability for any values of $L$ and $b_M L_1$.

Using this procedure, some values of the gains have been calculated, and they are shown in Table 1. For these calculations, we selected $b_m = k_{I1} = 1$, $k_{I2} = k_{I3} = k_{I4} = 0$, $\frac{1}{L} = 1.1$, and $L_1 = 0$.

It is important to mention that if a set of gains is useful to stabilize the origin of (9), in presence of an uncertainty/disturbance with a bound $L$ from (11), this controller can handle disturbances with a different bound $\hat{L}$ by scaling the gains.

# 5 | SIMULATION STUDY AND EXPERIMENTAL VALIDATION

In order to illustrate the performance of the presented algorithm, a simulation study was performed using the model of the RWP described in the previous Sections. Experiments have been carried out in a laboratory-scale RWP system developed in the Institut für Regelungs- und Automatisierungstechnik of TU Graz, Austria, and illustrated in Figure 1. The experiments were performed using Matlab Simulink over a data-acquisition board connected to the RWP system. The system's parameters for the experimental set-up, given in Table 2, were obtained with an off-line identification algorithm. They were also used for the simulations.

The experimental set-up can measure the positions of the pendulum and the wheel. To estimate the velocities $x_2$ and $x_4$, a second-order robust exact differentiator[23] was implemented. Since the control signal is not the torque (as assumed for the mathematical model), but voltage applied to the motor driving the wheel, the following relation between these two variables has been obtained experimentally

$$V = -0.2778\tau + 3.6 \times 10^{-4} x_4 .$$

We assume that the motor is much faster than the dynamics of the RWP, so that it is not necessary to take into account its dynamics. Note also that this control voltage signal has a range of $[-0.9, 0.9]$ Volts, and saturates at 0.9 [V].

| Name | Description | Units |
|------|-------------|-------|
| $\overline{m}$ | Equivalent mass of the system | 0.22 (kgm) |
| $d_{11}$ | Equivalent moment of inertia of the system | 0.0479 (kgm$^2$) |
| $J_2$ | Moment of inertia of the wheel | 0.0027 (kgm$^2$) |
| $b_2$ | Friction coefficient of the wheel | 0.015 (Ns/m$^2$) |
| $g$ | Acceleration of the gravity | 9.81 (m/sec$^2$) |

**TABLE 2** Parameters of the lab-scale reaction wheel pendulum system
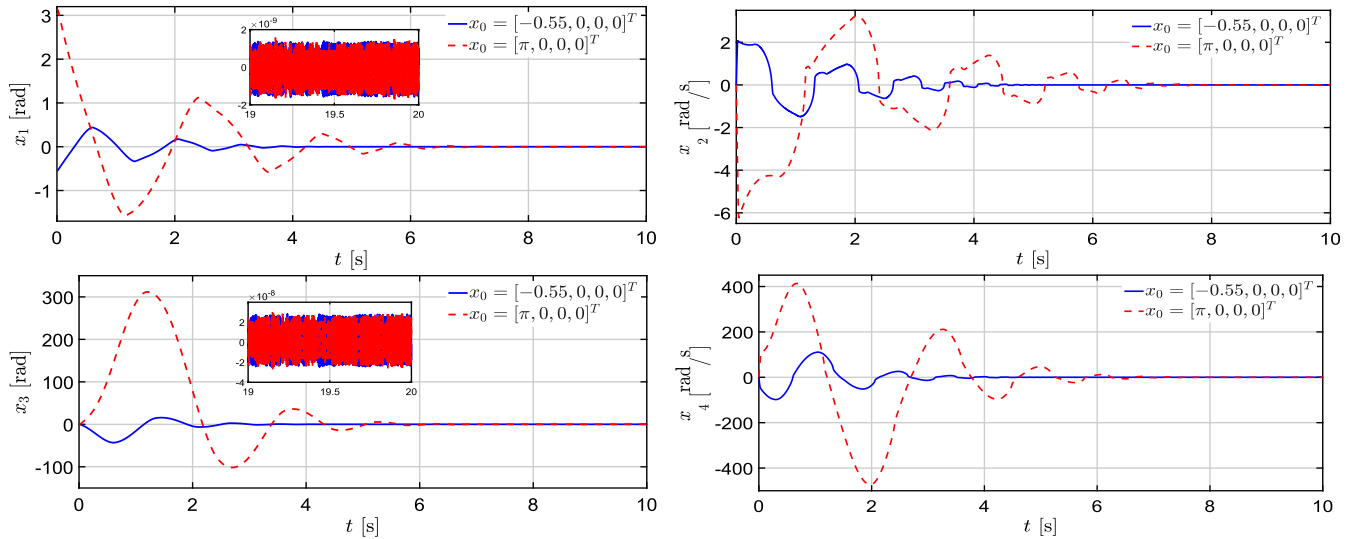


**FIGURE 2** States in the stabilization simulations [Colour figure can be viewed at wileyonlinelibrary.com]

## 5.1 | Simulation results

The control (4) with (2) and the 4-DIA described by (12) with $\kappa_1 = 422$, $\kappa_2 = 177.5$, $\kappa_3 = 56$ ($k_1 = k_2 = 2$, $k_3 = 5$), $k_4 = 45$, $k_{I1} = 8$, $k_{I2} = k_{I3} = k_{I4} = 0$ and scaling gain of $\lambda = 0.2$, were implemented in Matlab-Simulink. For the simulation, the fixed-step integration method of Runge-Kutta, with step time equal to $1 \times 10^{-4}[s]$, was used.

A *stabilization* scenario was first run, that is, $r(t) \equiv 0$, with an unbounded perturbation $\varphi_2(t, e) = 0.1 \sin(t) + 0.1t + 0.5$ and an uncertain control coefficient $\beta(t, e) = 2.5 + \sin(e_1) + \cos(e_2)$. Two initial conditions (given in terms of $x$) were used for the simulations, $x_{0,1} = [-1, 0, 0, 0]^T$ and $x_{0,2} = [\pi, 0, 0, 0]^T$. Since our results assure only local finite-time stability, the second initial condition $x_{0,2}$, which corresponds to the down-ward position of the pendulum, is a hard test for the algorithm, since it is very far away from the origin. In fact, to arrive at the origin from this initial condition, the point of singularity has to be crossed, and our analysis cannot assure the convergence. The results are shown in Figures 2 to 4, where the plant's variables $x$ are represented. Note that the origin is attained from both initial conditions. As commented before, it is surprising that this is achieved also when the pendulum starts in the downward position.

Figure 3 illustrates how the integral variable $\zeta$ converges in finite-time to the negative value of the unbounded perturbation $\varphi_2$, what explains why the 4-DIA is able to fully compensate it in the closed-loop. Figure 4 shows the control signal generated by the algorithm, which is *continuous*.

A *tracking* scenario has been also implemented. An integral gain of $k_{I1} = 0.1$ was used. The rest of the simulation parameters, including also the uncertain coefficient and the perturbation $\varphi_2$, are identical to the ones used for the stabilization scenario. The reference to be tracked was selected such that $x_1(t) = r_3(t) = 0.25 \sin(1.8t)$. The initial condition was selected as $x_0 = [0, 0, 0, 0]^T$. The results are shown in Figures 5 to 7. The pendulum position follows the desired reference and the errors stay close the origin despite the disturbance and the uncertain control coefficient. Note again that the generated control signal is continuous.
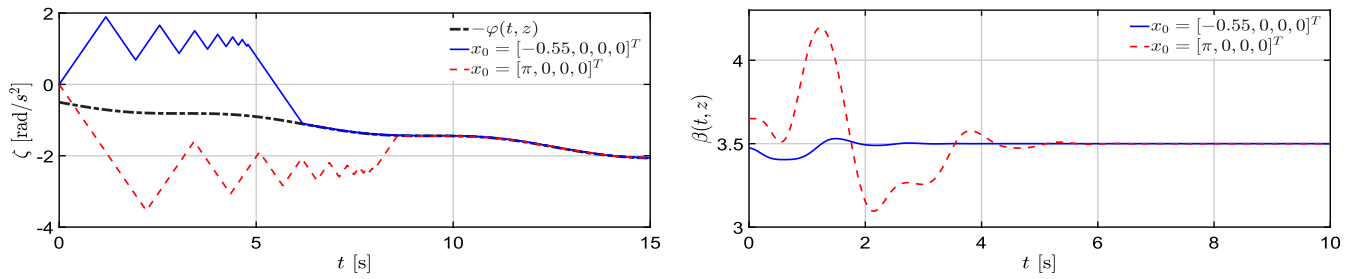
**FIGURE 3** Perturbation identification and uncertain control coefficient in the stabilization simulations [Colour figure can be viewed at wileyonlinelibrary.com]

**FIGURE 4** Control signal in the stabilization simulations [Colour figure can be viewed at wileyonlinelibrary.com]
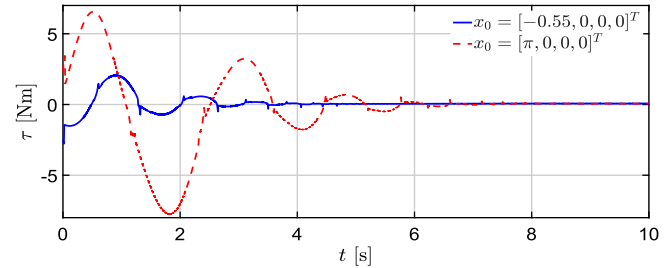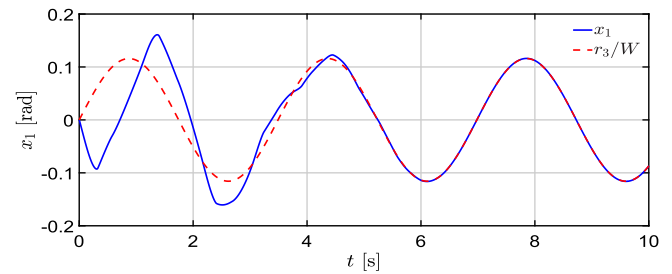


**FIGURE 5** Pendulum position in the tracking simulation [Colour figure can be viewed at wileyonlinelibrary.com]



## 5.2 | Experimental validation

The control (4) with (2) and the 4-DIA described by (12) were implemented in the real RWP system. The selected gains were $\kappa_1 = 13\,500$, $\kappa_2 = 5680$, $\kappa_3 = 1790$ ($k_1 = k_2 = 2$, $k_3 = 20$), $k_4 = 55$, $k_{I1} = 0.3$ $k_{I2} = k_{I3} = k_{I4} = 0$ and scaling $\lambda = 0.09$. As integration method the fixed-step Runge-Kutta algorithm was used, with step time $1 \times 10^{-4}$ [s].

A *stabilization* scenario was implemented (with reference $r(t) \equiv 0$), starting from two initial conditions, $x_0 = [-0.55, 0, 0, 0]^T$ and $x_0 = [\pi, 0, 0, 0]^T$. They are similar to the ones in the simulation study, to check if the same behaviour of the simulations is obtained. In the experiment, when the pendulum started in the downward position, the wheel position encoder was reset once the pendulum reached a position close to the origin. This was made in order to avoid that the controller perform large transients to bring the wheel position to zero. The results are shown in Figures 8 and 9. Figure 8 shows how the four states reach the origin and stay close to it, despite the discretization effects, or the presence of uncertainties, like dry friction, which cannot be fully compensated by a controller with continuous control signal.

Figure 9 shows the continuous torque signal generated by the 4-DIA, as well as the voltage that is the real control connected to the DC motor. Note that when the pendulum is performing the swing-up, the saturation limit is reached, so that the generated torque is not sufficient to swing the pendulum up in one step. This explains the oscillations produced by the 4-DIA, to be able to bring the pendulum to the upward position. This differs from the results obtained in simulations, where no saturation effect is considered, and the pendulum goes to the upward position in just one movement. These results show that the 4-DIA is capable of stabilizing all four states even with this saturation in the real control.

For the *tracking* scenario, the control (4) with (2), (6) and the 4-DIA described by (12) were implemented. The used gains were $\kappa_1 = 13\,500$, $\kappa_2 = 5680$, $\kappa_3 = 1790$ ($k_1 = k_2 = 2$, $k_3 = 20$), $k_4 = 59$, $k_{I1} = 0.2$ $k_{I2} = 1$, $k_{I3} = k_{I4} = 0$ and
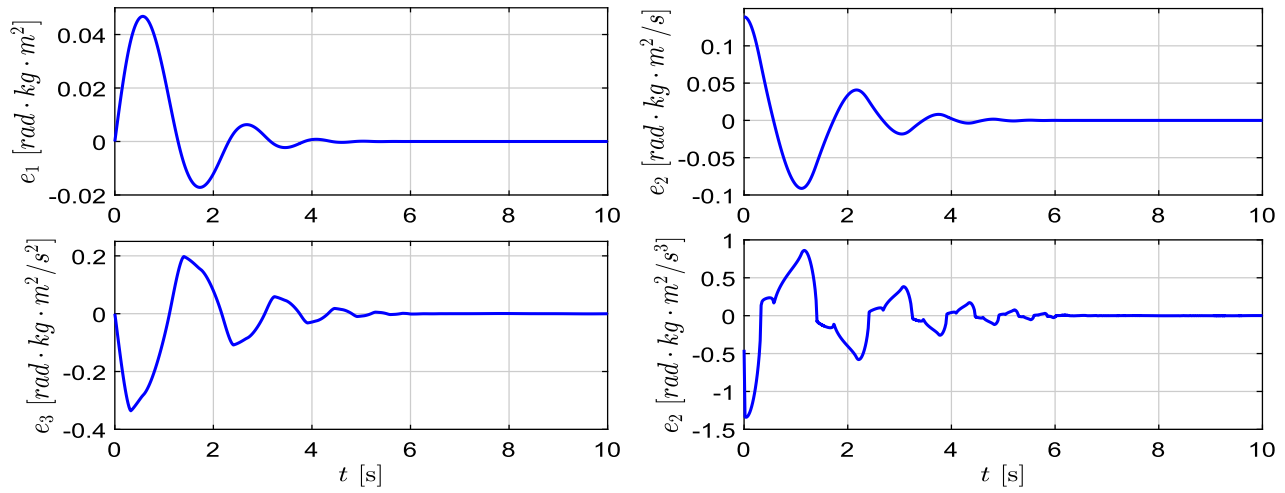
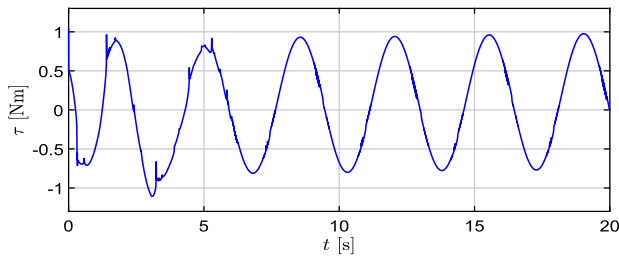**FIGURE 6** Errors in the tracking simulation [Colour figure can be viewed at wileyonlinelibrary.com]



**FIGURE 7** Control signal in the tracking simulation [Colour figure can be viewed at wileyonlinelibrary.com]
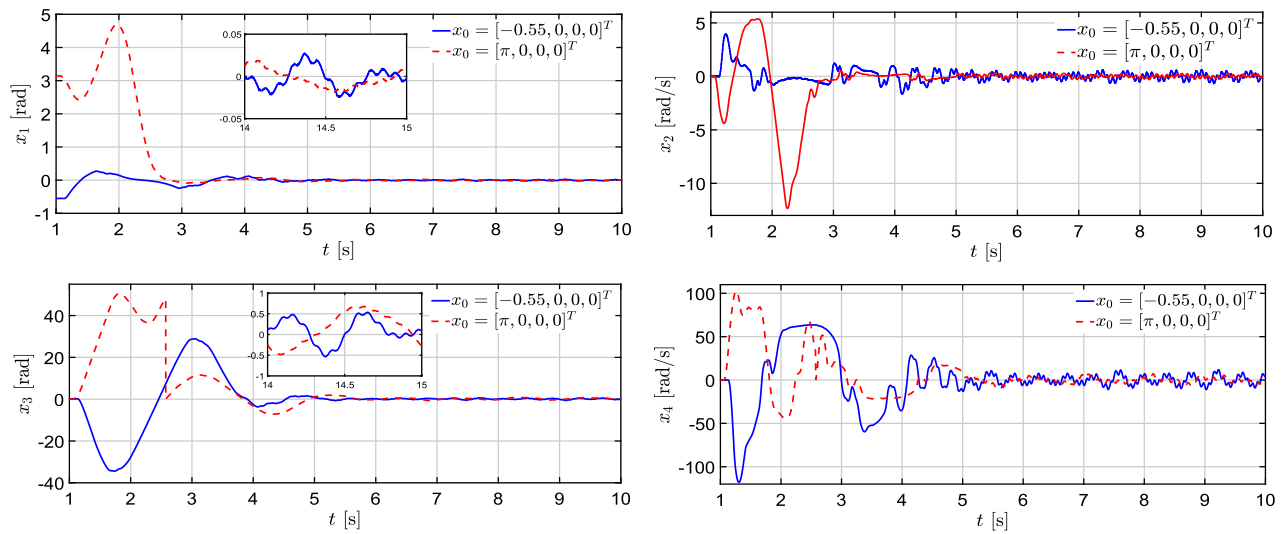


**FIGURE 8** States in the stabilization experiments [Colour figure can be viewed at wileyonlinelibrary.com]
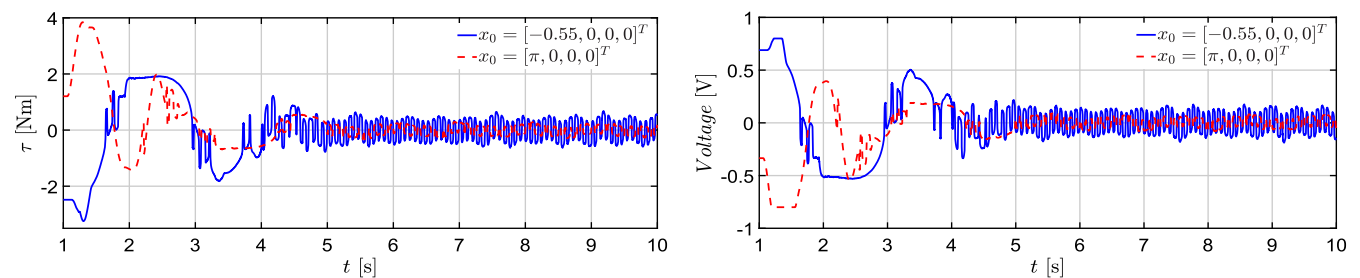


**FIGURE 9** Torque and voltage control signals in the stabilization experiments [Colour figure can be viewed at wileyonlinelibrary.com]

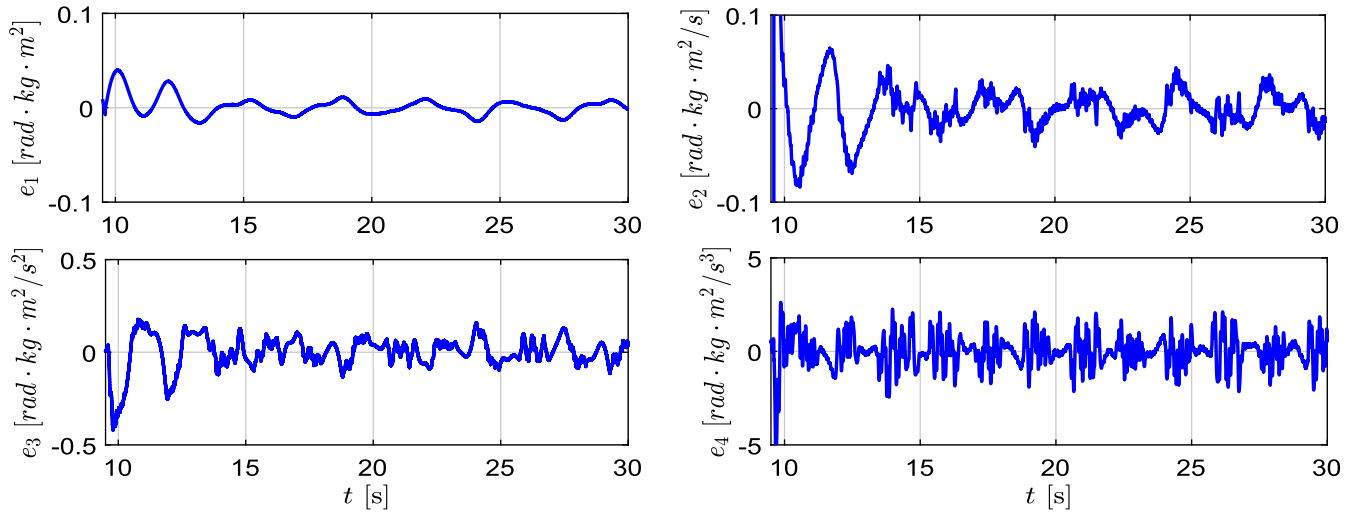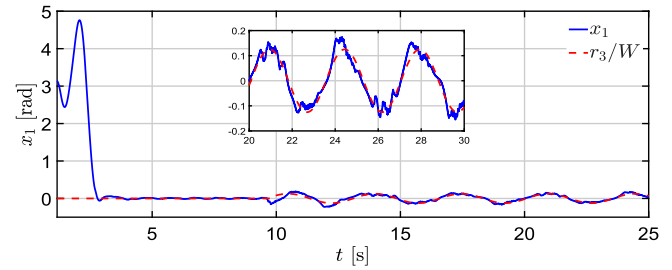**FIGURE 10** Pendulum position in the tracking experiment [Colour figure can be viewed at wileyonlinelibrary.com]



**FIGURE 11** Errors in the tracking experiment [Colour figure can be viewed at wileyonlinelibrary.com]
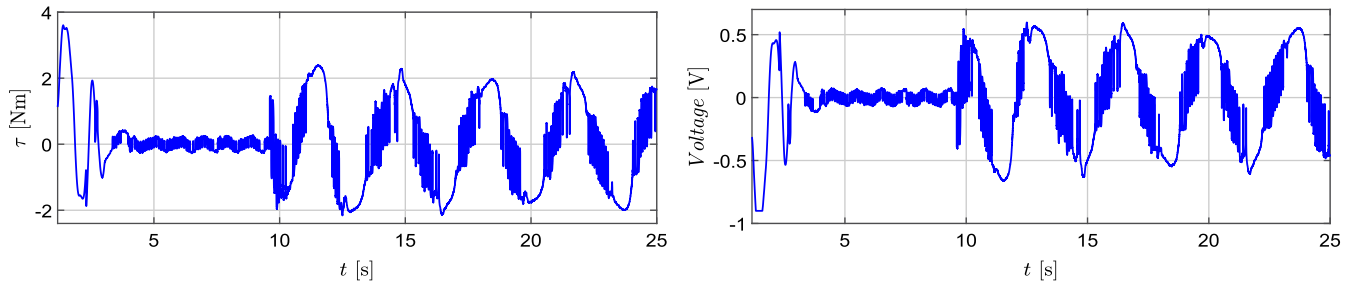


**FIGURE 12** Torque and voltage control signals in the tracking experiment [Colour figure can be viewed at wileyonlinelibrary.com]

scaling $\lambda = 0.25$. As integration method the fixed-step Runge-Kutta algorithm was used, with step time $1 \times 10^{-4}$ [s]. The pendulum was initiated in the downward position. For this reason, the reference signal was selected, such that during the first phase of the experiment (approx 9 seconds) a stabilization of the origin was intended, and after this period a reference signal was chosen such that $x_1(t) = r_3(t) = 0.25 \sin(1.8t)$. The results are shown in Figures 10 to 12. The pendulum position follows the desired reference and the errors stay close to the origin. Also, the control signal generated is continuous.

A video of the performed experiments with the real RWP can be seen in the following link: https://youtu.be/E3zXno2lTDg. First, the stabilization of the origin with a disturbance on the pendulum is done, and then the tracking of the sinusoidal signal close to the origin is realized.

## 6 | PRECISION ANALYSIS

It is well-known that the asymptotic stability of an equilibrium is a robust property (see, eg, Reference 24), and so small perturbations or uncertainties will not destroy the stability properties. Moreover, the existence of a smooth Lyapunov
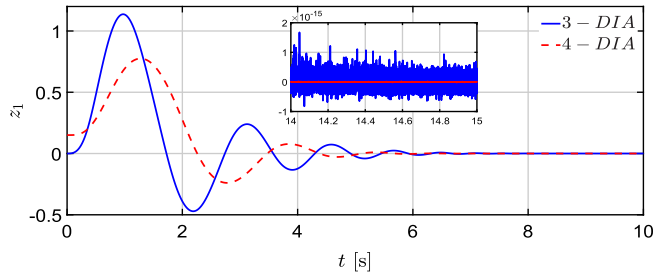
**FIGURE 13** Precision comparison in simulations [Colour figure can be viewed at wileyonlinelibrary.com]
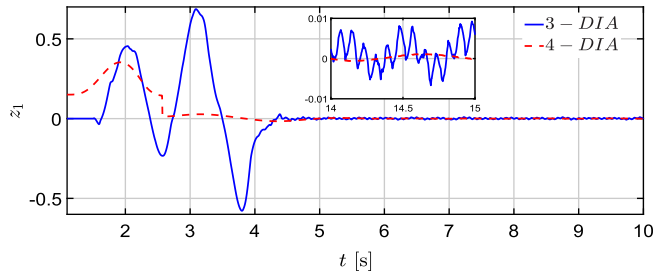


**FIGURE 14** Precision comparison in experiments [Colour figure can be viewed at wileyonlinelibrary.com]

Function permits to obtain enhanced robustness properties. So it is not surprising, that our algorithm, the 4-DIA, enjoys of such robustness properties. So, for example, small discretization errors, noise or delays will produce also small steady-state deviations from the equilibrium. For homogeneous systems these steady-state deviations (when small) can be expressed as powers of the amplitudes of the signals causing them (see, eg, Reference 25). The powers depend on the homogeneous weights of the variables involved. In the sliding-mode literature, they are usually referred to as the *precision* of the control scheme.

For the 4-DIA, it follows from this standard analysis,[25] that the theoretical precision for the states in steady-state are

$$|z_1| < \Delta_1 \overline{\tau}^5 , \quad |z_2| < \Delta_2 \overline{\tau}^4 , \quad |z_3| < \Delta_3 \overline{\tau}^3 , \quad |z_4| < \Delta_4 \overline{\tau}^2 , \quad |z_5| < \Delta_5 \overline{\tau} ,$$

where $\Delta_i > 0$, for $i = 1, \ldots, 5$, are constants depending on the gains, and $\overline{\tau}$ is the sample time.

In our previous work,[4] the stabilization of the RWP was done using a 3-DIA. In that case, only three states were considered $z_1, z_2, z_3$, since the position of the wheel was not taken into account for the stabilization. The theoretical precision of the 3-DIA is given by

$$|z_1| < \Delta_1 \overline{\tau}^4 , \quad |z_2| < \Delta_2 \overline{\tau}^3 , \quad |z_3| < \Delta_3 \overline{\tau}^2 .$$

Since for small values of $\overline{\tau}$ a higher power produces a smaller number, it is clear that the precision of the 3-DIA is smaller than that of the 4-DIA. Calculation of the coefficients $\Delta_i$ in the precision figures is very hard, so that we will use a simulation study to calculate them for both algorithms, the 3-DIA and the 4-DIA. This will allow us also to compare their precision.

We performed simulations of the stabilization of the origin, starting at the downward position, using a control coefficient $\beta(t, z) = 1$ and the same disturbance for both control algorithms, and Euler's integration method with fixed step. By changing the sample time $\overline{\tau}$, we obtained the following values:

$$3\text{-DIA:} \quad |z_1| < 2 \times 10^3 \overline{\tau}^4 , \quad |z_2| < 3 \times 10^2 \overline{\tau}^3 , \quad |z_3| < 3 \times 10^2 \overline{\tau}^2 ,$$

$$4\text{-DIA:} \quad |z_1| < 5 \times 10^5 \overline{\tau}^5 , \quad |z_2| < 8 \times 10^4 \overline{\tau}^4 , \quad |z_3| < 7 \times 10^3 \overline{\tau}^3 , \quad |z_4| < 2 \times 10^3 \overline{\tau}^2 .$$

It is clear that the 4-DIA has a higher precision than the 3-DIA. Figures 13 and 14 show the value of the state $z_1$ for each algorithm in simulations and experiments, respectively. These results confirm the theoretical and the numerical results obtained previously.

## 7 | DISCUSSION

In this section, we provide some interesting points of view of the obtained results of our article.

## 7.1 | RWP model used

We consider in this article for control design the full-order fourth-order model of the RWP system. This is an advantage compared to many works in the literature, as discussed in the introduction, where only a third-order model is used by neglecting the wheel position. We are able to also stabilize or regulate the wheel position, a much more challenging problem. Moreover, and also in contrast to many previous results, the control designed in this article takes into account realistic perturbations and uncertainties caused by, for example, parameter uncertainties. This renders our design more akin to a practical situation, and this explains partly the much better results obtained in the experiments.

## 7.2 | System performance

The result obtained in Theorem 1, is the local but *finite-time* stabilization of an equilibrium point or the *finite-time* tracking of a rather arbitrary (but small) reference. This is a much stronger property than the one provided by conventional controllers. On the one side, the convergence is in finite-time and not asymptotical or exponential, as usual. Furthermore, exact tracking in finite-time of arbitrary reference requires usually a much more complex controller, including for example an internal model of the desired tracking behaviour. In our case, a simple integral term can deal with a large class of perturbations and/or tracking signals. Finally, the precision, that is, steady state errors, as seen in Section 6, corresponds to the homogeneity weights of the variables, and is higher than with smooth controllers.

## 7.3 | Limitations

In this article, we only provide *local* stability results, and we do not analyze the effect on the region of attraction or performance of the saturation in the control signal. Nevertheless, despite these limitations in the analysis, the algorithm shows that it is able to perform, both in simulations and experiments, the swing-up and stabilization in one step. Further research is required to address both the global stabilization problem with and without saturated control.

## 8 | CONCLUSIONS

We have designed a *discontinuous* integral control law (DIA) to locally stabilize in finite-time an equilibrium or track an arbitrary but small reference signal for the full-order model of the RWP. The DIA fully counteracts matched perturbations which are Lipschitz continuous functions of time or unmatched uncertainties/perturbations that growth with the homogeneous norm of the states, for any growth constant, and an uncertain but positive and bounded control coefficient. We have shown that the model of the RWP with uncertain parameters and reference signal can be included in this uncertain model, and therefore the proposed controller solves the posed problem in a satisfactory way. To show the performance of the proposed control, a simulation study and an experimental verification have been carried out. This includes a study of the tracking precision achieved by the control algorithm. This study has also shown that the control algorithm is able to swing-up the pendulum from the downward position to the upward one. This is surprising and unexpected, since the proof only assures local stabilization/tracking.

The local results presented in this article can be easily extended to a much larger class of underactuated mechanical systems. For future works, we expect also to design *global* instead of *local* integral controllers for the RWP and some classes of underactuated mechanical systems.

**CONFLICT OF INTEREST**
The authors declare no potential conflict of interests.

## ORCID

*Diego Gutiérrez-Oribio* 🄳 https://orcid.org/0000-0002-5895-3416
*Ángel Mercado-Uribe* 🄳 https://orcid.org/0000-0002-7286-0814
*Jaime A. Moreno* 🄳 https://orcid.org/0000-0002-2556-9784
*Leonid Fridman* 🄳 https://orcid.org/0000-0003-0208-3615

## REFERENCES

1. Spong M, Corke P, Lozano R. Nonlinear control of the reaction wheel pendulum. *Automatica*. 2001;37:1845-1851.
2. Andrievsky B. Global stabilization of the unstable reaction-wheel pendulum. *Autom Remote Control*. 2011;72(9):1981-1993.
3. Estrada MA, Mendoza-Avila J, Moreno JA, Fridman L. Homogeneous control and finite-time stabilization of a reaction wheel pendulum system. Paper presented at: Proceedings of the Congreso Nacional de Control Automático; 2017:Monterrey, México.
4. Gutiérrez-Oribio D, Mercado-Uribe JA, Moreno JA, Fridman L. Stabilization of the reaction wheel pendulum via a third order discontinuous integral sliding mode algorithm. Paper presented at: Proceedings of the 15th International workshop on Variable Structure Systems; 2018; Graz, Austria.
5. Ortega R, Spong M, Gomez-Estern F, Blankenstein G. Stabilization of a class of underactuated mechanical systems via interconnection and damping assignment. *IEEE Trans Autom Control*. 2002;47(8):1218-1233.
6. Srinivas K, Behera L. Swing-up control strategies for a reaction wheel pendulum. *Int J Syst Sci*. 2008;39(12):1165-1177.
7. Iriarte R, Aguilar LT, Fridman L. Second order sliding mode tracking controller for inertia wheel pendulum. *J Frankl Inst*. 2013;350:92-106.
8. Shtessel Y, Edwards C, Fridman L, Levant A. *Sliding Mode Control and Observation*. Intuitive Theory of Sliding Mode Control. New York, NY: Birkhauser; 2014.
9. Boubaker O, Iriarte R, eds. *The Inverted Pendulum in Control Theory and Robotics: From Theory to New Innovations*. London, UK: IET; 2018.
10. Estrada A, Aguilar LT, Iriarte R, Fridman L. Two relay controller for real time trajectory generation and its application to inverted orbital stabilization of inertia wheel pendulum via quasi-continuous HOSM. *Asian J Control*. 2012;14(1):58-66.
11. Khalil H. *Nonlinear Systems*. Prentice Hall: Upper Saddle River, NJ; 1996.
12. Kamal S, Moreno J, Chalanga A, Bandyopadhyay B, Fridman L. Continuous terminal sliding-mode controller. *Automatica*. 2016;69:308-314.
13. Laghrouche S, Harmouche M, Chitour Y. Higher order super-twisting for perturbed chains of integrators. *IEEE Trans Autom Control*. 2017;62(7):3588-3593.
14. Moreno JA. Chapter 8 Discontinuous Integral Control for Systems with relative degree two. In: Julio C, Wen Y, eds. *New Perspectives and Applications of Modern Control Theory*. Cham: Springer International Publishing; 2018.
15. Torres-González V, Sanchez T, Fridman LM, Moreno JA. Design of continuous twisting algorithm. *Automatica*. 2017;80:119-126.
16. Mercado-Uribe JA, Moreno JA. Discontinuous integral action for arbitrary relative degree in sliding-mode control. *Automatica*. 2020;118:109018.
17. Pérez-Ventura U, Fridman L. When it is reasonable to implement the discontinuous sliding-mode controllers instead of the continuous ones: frequency domain criteria. *Int J Robust Nonlinear Control*. 2019;29(3):810-828.
18. Levant A. Sliding order and sliding accuracy in sliding mode control. *Int J Control*. 1993;58:1247-1263.
19. Levant A. Robust exact differentiation via sliding mode technique. *Automatica*. 1998;34(3):379-384.
20. Mendoza-Ávila J, Moreno JA, Fridman L. An idea for Lyapunov function design for arbitrary order continuous twisting algorithm. Paper presented at: Proceedings of the IEEE 56th Annual Conference on Decision and Control; 2017; Melbourne, Australia.
21. Moreno J. Discontinuous integral control for mechanical systems. Paper presented at: Proceedings of the 14th International Workshop on Variable Structure Systems; 2016; Nanjing, China.
22. Spong M, Vidyasagar M. *Robot Dynamics and Control*. New York, NY: Wiley; 1989.
23. Levant A. Higher-order sliding modes, differentiation and output-feedback control. *Int J Control*. 2008;76(9/10):924-941.
24. Baccioti A, Rosier L. *Lyapunov Functions and Stability in Control Theory*. 2nd ed. New York, NY: Springer-Verlag; 2005.
25. Levant A. Homogeneity approach to high-order sliding mode design. *Automatica*. 2005;41(5):823-830.
26. Andrieu V, Praly L, Astolfi A. Homogeneous aproximation, recursive observer design and output feedback. *SIAM J Control Optim*. 2008;47(4):1814-1850.
27. Cruz-Zavala E, Moreno JA. Homogeneous high order sliding mode design: a Lyapunov approach. *Automatica*. 2017;80:232-238.
28. Mercado-Uribe JA, Moreno JA. Discontinuous integral control for systems in controller form. Paper presented at: Proceedings Congreso Nacional de Control Automático; 2017; Monterrey, México.

## APPENDIX A. HOMOGENEITY

For a vector $x = (x_1, \ldots, x_n) \in \mathbb{R}^n$, the *dilation operator* is the family of linear transformations defined by $\Delta_\epsilon^{\mathbf{r}} x = (\epsilon^{r_1} x_1, \ldots, \epsilon^{r_n} x_n)$, $\forall \epsilon > 0$. For $i = 1, \ldots, n$, $r_i > 0$ is the *weight* of the component $x_i$ and $\mathbf{r} = (r_1, \ldots, r_n)$ is the vector of weights. A function $V : \mathbb{R}^n \to \mathbb{R}$ (respectively, a vector field $f : \mathbb{R}^n \to \mathbb{R}^n$, or vector-set $F(x) \subset \mathbb{R}^n$) is called $\mathbf{r}$-homogeneous of *degree* $m \in \mathbb{R}$ if for all $x \in \mathbb{R}^n$ and all $\epsilon > 0$ $V(\Delta_\epsilon^{\mathbf{r}} x) = \epsilon^m V(x)$ holds (respectively, $f(\Delta_\epsilon^{\mathbf{r}} x) = \epsilon^m \Delta_\epsilon^{\mathbf{r}} f(x)$, $F(\Delta_\epsilon^{\mathbf{r}} x) = \epsilon^m \Delta_\epsilon^{\mathbf{r}} F(x)$).[21,24]

For a given vector $\mathbf{r}$, the homogeneous norm is defined by $\|x\|_{\mathbf{r}, p} := \left( \sum_{i=1}^n |x_i|^{\frac{p}{r_i}} \right)^{\frac{1}{p}}$, $\forall x \in \mathbb{R}^n$, for any $p \geq 1$. The set $S = \{x \in \mathbb{R}^n : \|x\|_{\mathbf{r}, p} = 1\}$ is the homogeneous unit sphere.[24]

### A.1 Some properties of homogeneous functions

Let $V_1$ and $V_2$ two continuously differentiable $\mathbf{r}$-homogeneous functions (respectively, a vector field $f_1$) of degree $m_1$, $m_2$ (respectively, $l_1$), then:[24]

(i) $V_1 V_2$ is homogeneous of degree $m_1 + m_2$,
(ii) There exist a constant $c_1 > 0$, such that $V_1 \leq c_1 \|x\|_{\mathbf{r},p}^{m_1}$, moreover if $V_1$ is positive definite, there exists $c_2$ such that $V_1 \geq c_2 \|x\|_{\mathbf{r},p}^{m_1}$,
(iii) $\partial V_1(x)/\partial x_i$ is homogeneous of degree $m_1 - r_i$,
(iv) $L_f V_1(x)$, the Lie derivative of $V_1$ along $f$, is homogeneous of degree $m_1 + l_1$.

The following property of *continuous* homogeneous functions is well-known.

**Lemma 1** (21,26). *Let $\eta : \mathbb{R}^n \to \mathbb{R}$ and $\gamma : \mathbb{R}^n \to \mathbb{R}$ two homogeneous and continuous functions, with the same weights $\mathbf{r} = (r_1, \ldots, r_n)$ and degree $m$. Let $\gamma(x) \geq 0$ for all $x \in \mathbb{R}^n$ and suppose that*

$$\{x \in \mathbb{R}^n \setminus \{0\} | \gamma(x) = 0\} \subseteq \{x \in \mathbb{R}^n \setminus \{0\} | \eta(x) > 0\} .$$

*Then, there exists a real number $\lambda^*$ so that, for all $\lambda > \lambda^*$, for all $x \in \mathbb{R}^n \setminus \{0\}$ and for some $c > 0$, it is true that*

$$\eta(x) + \lambda \gamma(x) \geq c \|x\|_{\mathbf{r},p}^m .$$

The previous Lemma 1 requires the functions to be *continuous*. The following lemma, proven in Reference 27, extends this result to *semi-continuous* functions. This permits to handle multivalued functions.

**Lemma 2** (27). *Let $\eta : \mathbb{R}^n \to \mathbb{R}$ and $\gamma : \mathbb{R}^n \to \mathbb{R}$ two homogeneous and lower semi-continuous single-valued functions, with the same weights $\mathbf{r} = (r_1, \ldots, r_n)$ and degree $m$. Let $\gamma(x) \geq 0$ for all $x \in \mathbb{R}^n$ and suppose that*

$$\{x \in \mathbb{R}^n \setminus \{0\} | \gamma(x) = 0\} \subseteq \{x \in \mathbb{R}^n \setminus \{0\} | \eta(x) > 0\} .$$

*Then there exists a real number $\lambda^*$ so that, for all $\lambda > \lambda^*$, for all $x \in \mathbb{R}^n \setminus \{0\}$ and for some $c > 0$, it is true that*

$$\eta(x) + \lambda \gamma(x) \geq c \|x\|_{\mathbf{r},p}^m .$$

We will make use of the following property of the "power-signed" function $\lceil x \rfloor^\beta$, $\beta > 0$, which is a consequence of its monotonicity: For any real numbers $x \neq y \in \mathbb{R}$, $(\lceil x + y \rfloor^\beta - \lceil x \rfloor^\beta) x > 0$. As a consequence

$$\text{sign} \left( \lceil x + y \rfloor^\beta - \lceil y \rfloor^\beta \right) = \text{sign} (x), \quad \beta > 0.$$

## APPENDIX B. PROOF OF THEOREM 1

The dynamics of the closed-loop system consisting of the (transformed) model of the RWP (9) and the 4-DIA (12), which is given by (13), can be rewritten in the following form

$$\dot{e}_1 = e_2,$$
$$\dot{e}_2 = W e_3 + W \psi(t, e_3),$$

$$\dot{e}_3 = e_4,$$

$$\dot{e}_4 = -k_4\beta(t, e)\left[\left[k_3^{\frac{5}{2}}k_2^{\frac{5}{3}}k_1^{\frac{5}{4}}e_1 + k_3^{\frac{5}{2}}k_2^{\frac{5}{3}}\lceil e_2\rfloor^{\frac{5}{4}} + k_3^{\frac{5}{2}}\lceil e_3\rfloor^{\frac{5}{3}} + \lceil e_4\rfloor^{\frac{5}{2}}\right]^{\frac{1}{5}} - e_5 - \tilde{\varphi}_1(t, e)\right],$$

$$\dot{e}_5 \in -\tilde{k}_{I1}\left[\left[e_1 + k_{I2}\lceil e_2\rfloor^{\frac{5}{4}} + k_{I3}\lceil e_3\rfloor^{\frac{5}{3}} + k_{I4}\lceil e_4\rfloor^{\frac{5}{2}}\right]^0 + [-\overline{L}, \overline{L}]\right],$$

$$e_5 := \frac{\zeta + \varphi_2(t, e)}{k_4}, \quad \tilde{\varphi}_1(t, e) := \frac{\varphi_1(t, e)}{k_4}, \quad \tilde{k}_{I1} = \frac{k_{I1}}{k_4}, \quad \overline{L} = \frac{L}{k_{I1}}. \tag{B1}$$

where we have introduced a modified integral variable $e_5 = \frac{\zeta + \varphi_2(t, e)}{k_4}$, consisting of the sum of the integral variable $\zeta$ and the nonvanishing perturbation term $\varphi_2(t, e)$. Here $\overline{L} = \frac{L}{k_{I1}}$ and we have used the assumed bound on the derivative of $\varphi_2(t, e)$ given in (11). Moreover, we have employed the following relations between the controller gains $\kappa_1, \kappa_2, \kappa_3$ and the gains $k_1, k_2, k_3$

$$\kappa_1 = k_3^{\frac{5}{2}}k_2^{\frac{5}{3}}k_1^{\frac{5}{4}}, \quad \kappa_2 = k_3^{\frac{5}{2}}k_2^{\frac{5}{3}}, \quad \kappa_3 = k_3^{\frac{5}{2}},$$

which will be utilized in the following calculations. Note also that we have set the scaling parameter $\lambda = 1$. We will perform the proof first with $\lambda = 1$, for *some* value of $L$, and then we show that with the scaling parameter $\lambda$, it is possible to achieve stability for an arbitrary value of $L$.

System (B1), without considering the two uncertain/perturbation terms $\psi(t, e_3)$ and $\varphi_1(t, e)$, is **r**-homogeneous of degree $d = -1$ and weights $\mathbf{r} = (r_1, r_2, r_3, r_4, r_5) = (5, 4, 3, 2, 1)$ for each of the states $e_1, \ldots, e_5$.

We will show that, in the absence of the term $\psi(t, e_3)$, system (B1) has an equilibrium $e = 0$ Globally Asymptotically Stable, and because of its negative homogeneity degree, it is thus globally finite-time stable. When $\psi(t, e_3)$ is present, only local finite-time stability is attained. We divide the proof of the theorem in several parts:

1. We propose a homogeneous Lyapunov function (LF) candidate, and we show that it is differentiable, positive definite, and radially unbounded.
2. We show that, in the absence of the both terms $\psi(t, e_3)$ and $\varphi_1(t, e)$, its derivative is globally negative definite by selecting appropriately the gains of the controller. We specify the procedure to determine these gains.
3. We consider the effect of the vanishing uncertain term $\varphi_1(t, e)$ and show that the derivative of the LF remains globally negative definite if the growth of $\varphi_1(t, e)$ satisfies the condition in (11). We analyze the effect of this perturbation in the gains.
4. We consider the effect of the term $\psi(t, e_3)$ and show that, if the condition in (11) is fulfilled, the derivative of the LF is only *locally* negative definite.
5. Finally, we show how can we scale the gains of the controller to maintain the stability.

## B.1 The homogeneous Lyapunov function candidate

Consider the following **r**-homogeneous Lyapunov function (LF) candidate $\mathcal{V}(e)$ of degree $m$ (obtained as in Reference 28)

$$\mathcal{V}(e) = \gamma_3 V_3(\xi_1, e_2, e_3) + \frac{2}{m}|e_4|^{\frac{m}{2}} + k_3^{\frac{m-2}{2}}\left[\lceil e_3\rfloor^{\frac{5}{3}} + k_2^{\frac{5}{3}}\lceil e_2\rfloor^{\frac{5}{4}} + k_2^{\frac{5}{3}}k_1^{\frac{5}{4}}\xi_1\right]^{\frac{m-2}{5}}e_4$$

$$+ \left(1 - \frac{2}{m}\right)k_3^{\frac{m}{2}}\left|\lceil e_3\rfloor^{\frac{5}{3}} + k_2^{\frac{5}{3}}\lceil e_2\rfloor^{\frac{5}{4}} + k_2^{\frac{5}{3}}k_1^{\frac{5}{4}}\xi_1\right|^{\frac{m}{5}} + \frac{1}{m}|e_5|^m,$$

$$V_3(\xi_1, e_2, e_3) = \gamma_2 V_2(\xi_1, e_2) + \frac{3}{m}|e_3|^{\frac{m}{3}} + k_2^{\frac{m-3}{3}}\left[\lceil e_2\rfloor^{\frac{5}{4}} + k_1^{\frac{5}{4}}\xi_1\right]^{\frac{m-3}{5}}e_3 + \left(1 - \frac{3}{m}\right)k_2^{\frac{m}{3}}\left|\lceil e_2\rfloor^{\frac{5}{4}} + k_1^{\frac{5}{4}}\xi_1\right|^{\frac{m}{5}},$$

$$V_2(\xi_1, e_2) = \gamma_1\frac{5}{m}|\xi_1|^{\frac{m}{5}} + \frac{4}{m}|e_2|^{\frac{m}{4}} + k_1^{\frac{m-4}{4}}\lceil\xi_1\rfloor^{\frac{m-4}{5}}e_2 + \left(1 - \frac{4}{m}\right)k_1^{\frac{m}{4}}|\xi_1|^{\frac{m}{5}},$$

where

$$\xi_1 = e_1 - k_\xi\lceil e_5\rfloor^5, \quad k_\xi = k_3^{-\frac{5}{2}}k_2^{-\frac{5}{3}}k_1^{-\frac{5}{4}}, \quad \dot{\xi}_1 = e_2 - 5k_\xi|e_5|^4\dot{e}_5.$$

We will show that $\mathcal{V}(e)$ is positive definite for any positive constants $\gamma_1,\ \gamma_2,\ \gamma_3 > 0$. Note that it is required to have the degree $m \geq 9$ for the powers in $\mathcal{V}(e)$ to be larger than one, i.e. for making $\mathcal{V}(e)$ differentiable everywhere. Now we procede to show that $\mathcal{V}(e)$ is positive definite and radially unbounded for *any* $\gamma_1 > 0$, $\gamma_2 > 0$, and $\gamma_3 > 0$.

- Note that $\gamma_1 \frac{5}{m} |\xi_1|^{\frac{m}{5}}$, which is the first term in $V_2(\xi_1,\ e_2)$, is positive $\gamma_1 \frac{5}{m} |\xi_1|^{\frac{m}{5}} \geq 0$ and it is zero only when $\xi_1 = 0$. In this case, we have that $V_2(0,\ e_2) = \frac{4}{m} |e_2|^{\frac{m}{4}} \geq 0$, which is positive, except when $e_2 = 0$. Since $V_2(\xi_1,\ e_2)$ is continuous and homogeneous, Lemma 1 implies that selecting $\gamma_1 > 0$ sufficiently large function $V_2(\xi_1,\ e_2)$ is positive definite (in its two variables). In fact, using Young's inequality, it is possible to show that with $\gamma_1 = 0$ $V_2$ is positive semidefinite. This implies that $V_2$ is positive definite for any $\gamma_1 > 0$.

- The first term in $V_3(\xi_1,\ e_2,\ e_3)$ is $V_2(\xi_1,\ e_2)$, which is positive definite, and so it vanishes only when $(\xi_1,\ e_2) = 0$. When this happens $V_3(0,\ 0,\ e_3) = \frac{3}{m} |e_3|^{\frac{m}{3}} \geq 0$, which is positive, except for $e_3 = 0$. Again, Lemma 1 implies that selecting $\gamma_2 > 0$ sufficiently large function $V_3(\xi_1,\ e_2,\ e_3)$ becomes positive definite (in its three variables). Again, Young's inequality shows that $V_3 \geq 0$ when $\gamma_2 = 0$. Thus, $V_3$ is positive definite for any $\gamma_2 > 0$.

- Finally, the first term in $\mathcal{V}(e)$ is $V_3(\xi_1,\ e_2,\ e_3)$, which is positive definite, and so it vanishes only when $(\xi_1,\ e_2,\ e_3) = 0$. When this happens $\mathcal{V}|_{(\xi_1,\ e_2,\ e_3)=0} = \frac{2}{m} |e_4|^{\frac{m}{2}} + \frac{1}{m} |e_5|^m \geq 0$, which is positive, except for $e_4 = e_5 = 0$. Again, Lemma 1 implies that selecting $\gamma_3 > 0$ sufficiently large function $\mathcal{V}(e)$ becomes positive definite (in its five variables). Once more, Young's inequality shows that $V_4 \geq 0$ when $\gamma_3 = 0$. Thus, $\mathcal{V}$ is positive definite for any $\gamma_3 > 0$

Moreover, $\mathcal{V}(e)$ being homogeneous and positive definite is also radially unbounded. And thus it is an appropriate LF candidate.

## B.2 The derivative of $\mathcal{V}(e)$
The derivative of $\mathcal{V}(e)$ along the trajectories of (B1) is given by

$$\dot{\mathcal{V}}(e) = -\mathcal{W}(e) + \beta(t,\ e)C_4^{(1)}\varphi_1(t,\ e) + WC_2^{(1)}\psi(t,\ e_3), \tag{B2}$$

where

$$\mathcal{W}(e) = k_4\beta(t,\ e)C_4^{(1)}(e)F_1(e) + G_1(e), \tag{B3}$$

and

$$G_1(e) = -C_1^{(1)}(e)e_2 - WC_2^{(1)}(e)e_3 - C_3^{(1)}(e)e_4$$
$$+ \tilde{k}_{I1}C_5^{(1)}(e)\left[\left\lceil \xi_1 + k_\xi \lceil e_5 \rfloor^5 + k_{I2}\lceil e_2 \rfloor^{\frac{5}{4}} + k_{I3}\lceil e_3 \rfloor^{\frac{5}{3}} + k_{I4}\lceil e_4 \rfloor^{\frac{5}{2}} \right\rfloor^0 + [-\overline{L},\ \overline{L}]\right],$$

$$F_1(e) = \left\lceil k_3^{\frac{5}{2}} k_2^{\frac{5}{3}} k_1^{\frac{5}{4}} \xi_1 + k_3^{\frac{5}{2}} k_2^{\frac{5}{3}} \lceil e_2 \rfloor^{\frac{5}{4}} + k_3^{\frac{5}{2}} \lceil e_3 \rfloor^{\frac{5}{3}} + \lceil e_4 \rfloor^{\frac{5}{2}} + \lceil e_5 \rfloor^5 \right\rfloor^{\frac{1}{5}} - e_5,$$

$$C_1^{(1)}(e) = \gamma_2\gamma_3\left[\gamma_1\lceil \xi_1 \rfloor^{\frac{m-5}{5}} + \frac{m-4}{5}k_1^{\frac{m-4}{4}}|\xi_1|^{\frac{m-9}{5}}\left(e_2 + k_1\lceil \xi_1 \rfloor^{\frac{4}{5}}\right)\right]$$
$$+ \gamma_3\frac{m-3}{5}k_1^{\frac{5}{4}}k_2^{\frac{m-3}{3}}\left(e_3 + k_2\left\lceil \lceil e_2 \rfloor^{\frac{5}{4}} + k_1^{\frac{5}{4}}\xi_1 \right\rfloor^{\frac{3}{5}}\right)\left|\lceil e_2 \rfloor^{\frac{5}{4}} + k_1^{\frac{5}{4}}\xi_1\right|^{\frac{m-8}{5}}$$
$$+ \frac{m-2}{5}k_3^{\frac{m-2}{2}}k_2^{\frac{5}{3}}k_1^{\frac{5}{4}}\left|\lceil e_3 \rfloor^{\frac{5}{3}} + k_2^{\frac{5}{3}}\lceil e_2 \rfloor^{\frac{5}{4}} + k_2^{\frac{5}{3}}k_1^{\frac{5}{4}}\xi_1\right|^{\frac{m-7}{5}}\left(e_4 + k_3\left\lceil \lceil e_3 \rfloor^{\frac{5}{3}} + k_2^{\frac{5}{3}}\lceil e_2 \rfloor^{\frac{5}{4}} + k_2^{\frac{5}{3}}k_1^{\frac{5}{4}}\xi_1 \right\rfloor^{\frac{2}{5}}\right),$$

$$C_2^{(1)}(e) = \gamma_2\gamma_3\left(\lceil e_2 \rfloor^{\frac{m-4}{4}} + k_1^{\frac{m-4}{4}}\lceil \xi_1 \rfloor^{\frac{m-4}{5}}\right)$$
$$+ \gamma_3\frac{m-3}{4}k_2^{\frac{m-3}{3}}\left(e_3 + k_2\left\lceil \lceil e_2 \rfloor^{\frac{5}{4}} + k_1^{\frac{5}{4}}\xi_1 \right\rfloor^{\frac{3}{5}}\right)\left|\lceil e_2 \rfloor^{\frac{5}{4}} + k_1^{\frac{5}{4}}\xi_1\right|^{\frac{m-8}{5}}|e_2|^{\frac{1}{4}}$$
$$+ \frac{m-2}{4}k_3^{\frac{m-2}{2}}k_2^{\frac{5}{3}}\left|\lceil e_3 \rfloor^{\frac{5}{3}} + k_2^{\frac{5}{3}}\lceil e_2 \rfloor^{\frac{5}{4}} + k_2^{\frac{5}{3}}k_1^{\frac{5}{4}}\xi_1\right|^{\frac{m-7}{5}}\left(e_4 + k_3\left\lceil \lceil e_3 \rfloor^{\frac{5}{3}} + k_2^{\frac{5}{3}}\lceil e_2 \rfloor^{\frac{5}{4}} + k_2^{\frac{5}{3}}k_1^{\frac{5}{4}}\xi_1 \right\rfloor^{\frac{2}{5}}\right)|e_2|^{\frac{1}{4}},$$

$$C_3^{(1)}(e) = \gamma_3 \left( \lceil e_3 \rfloor^{\frac{m-3}{3}} + k_2^{\frac{m-3}{3}} \left\lceil \lceil e_2 \rfloor^{\frac{5}{4}} + k_1^{\frac{5}{4}} \xi_1 \right\rfloor^{\frac{m-3}{5}} \right)$$

$$+ \frac{m-2}{3} k_3^{\frac{m-2}{2}} \left\lceil \lceil e_3 \rfloor^{\frac{5}{3}} + k_2^{\frac{5}{3}} \lceil e_2 \rfloor^{\frac{5}{4}} + k_2^{\frac{5}{3}} k_1^{\frac{5}{4}} \xi_1 \right\rfloor^{\frac{m-7}{5}} \left( e_4 + k_3 \left\lceil \lceil e_3 \rfloor^{\frac{5}{3}} + k_2^{\frac{5}{3}} \lceil e_2 \rfloor^{\frac{5}{4}} + k_2^{\frac{5}{3}} k_1^{\frac{5}{4}} \xi_1 \right\rfloor^{\frac{2}{5}} \right) |e_3|^{\frac{2}{3}},$$

$$C_4^{(1)}(e) = \lceil e_4 \rfloor^{\frac{m-2}{2}} + k_3^{\frac{m-2}{2}} \left\lceil \lceil e_3 \rfloor^{\frac{5}{3}} + k_2^{\frac{5}{3}} \lceil e_2 \rfloor^{\frac{5}{4}} + k_2^{\frac{5}{3}} k_1^{\frac{5}{4}} \xi_1 \right\rfloor^{\frac{m-2}{5}},$$

$$C_5^{(1)}(e) = |e_5|^4 (\lceil e_5 \rfloor^{m-5} - 5k_\xi C_1^{(1)}(e)) .$$

Functions $C_1^{(1)}, \ldots, C_5^{(1)}$ and $F_1(e)$ are continuous and homogeneous. $G_1(e)$ is homogeneous, but it is a multivalued function, since it contains the interval $[-\overline{L}, \overline{L}]$, the uncertain $\beta$, and also the (multivalued) sign function $\lceil \cdot \rfloor^0$. A multivalued function has as image, for each point in the domain, a set, instead of a point, as it is the case for the usual single-valued functions.

In the rest of this subsection, we will show that the multivalued function $\mathcal{W}(e)$ is positive definite, if the gains of the controller are appropriately designed. For a multivalued function this means that for every point of the domain, that is, $\forall e \in \mathbb{R}^5 \setminus \{0\}$ the set of values attained by $\mathcal{W}(e)$ are positive, and $\mathcal{W}(0) = 0$. This will imply the Global Finite-Time stability of $e = 0$ in the absence of $\psi(t, e_3)$ and $\varphi_1(t, e)$.

The proof of this fact uses basically the property of homogeneous functions given in Lemma 1. However, this Lemma requires the functions to be continuous. Since $\mathcal{W}(e)$ is multivalued, we cannot use Lemma 1, but can resort to Lemma 2, which requires the functions to be semi-continuous. We will give here the basic reasons why we can use Lemma 2, but neither entering into the details nor giving the proofs. For this we refer the reader to Reference 27. The main facts are the following: (i) Function $\mathcal{W}(e)$ is a multivalued upper semi-continuous and bounded function. (ii) For such a function, there exists a single-valued lower semi-continuous function, say $\underline{\mathcal{W}}(e)$, such that $\mathcal{W}(e) \geq \underline{\mathcal{W}}(e)$. (iii) We can apply Lemma 2 to the function $\underline{\mathcal{W}}(e)$. (iv) If $\underline{\mathcal{W}}(e)$ is positive definite, it follows that also $\mathcal{W}(e)$ is positive definite. For simplicity, we will keep for the calculations the multivalued function $\mathcal{W}(e)$, but apply Lemma 2 to its lower semi-continuous lower bound $\underline{\mathcal{W}}(e)$ when necessary. This said, we can proceed with the proof. We will usually omit henceforth the dependence of these and other functions to avoid cluttering. The proof is done in several steps:

1. The first term in $\mathcal{W}(e)$ is $k_4 \beta(t, e) C_4 F_1$. We show that it is positive semidefinite. We do this by first showing that the continuous functions $C_4$ and $F_1$ vanish on the same set

$$S_1 = \left\{ e \in \mathbb{R}^5 | e_4 = -k_3 \left\lceil \lceil e_3 \rfloor^{\frac{5}{3}} + k_2^{\frac{5}{3}} \lceil e_2 \rfloor^{\frac{5}{4}} + k_2^{\frac{5}{3}} k_1^{\frac{5}{4}} \xi_1 \right\rfloor^{\frac{2}{5}} \right\} .$$

This follows from the simple calculations

$$C_4^{(1)}(e) = 0 \Leftrightarrow \lceil e_4 \rfloor^{\frac{m-2}{2}} + k_3^{\frac{m-2}{2}} \left\lceil \lceil e_3 \rfloor^{\frac{5}{3}} + k_2^{\frac{5}{3}} \lceil e_2 \rfloor^{\frac{5}{4}} + k_2^{\frac{5}{3}} k_1^{\frac{5}{4}} \xi_1 \right\rfloor^{\frac{m-2}{5}} = 0 \Leftrightarrow e \in S_1 \Leftrightarrow F_1(e) = 0 .$$

Moreover, evaluating at a point, for example, at $\xi_1 = e_2 = e_3 = e_5 = 0$, $F_1(0, 0, 0, e_4, 0) = \lceil e_4 \rfloor^{\frac{1}{2}}$ and $C_4^{(1)}(0, 0, 0, e_4, 0) = \lceil e_4 \rfloor^{\frac{m-2}{2}}$, we conclude that $C_4^{(1)}$ and $F_1$ have the same sign.

2. Evaluating $\mathcal{W}(e)$ on the set $S_1$ we obtain

$$\mathcal{W}|_{S_1} = \mathcal{F}(\xi_1, e_2, e_3) + \tilde{k}_{I1} H(\xi_1, e_2, e_3, e_5) , \tag{B4}$$

$$\mathcal{F}(\xi_1, e_2, e_3) = k_3 C_3^{(2)}(\xi_1, e_2, e_3) F_2(\xi_1, e_2, e_3) + G_2(\xi_1, e_2, e_3) \tag{B5}$$

where

$$F_2 = \left\lceil \lceil e_3 \rfloor^{\frac{5}{3}} + k_2^{\frac{5}{3}} \lceil e_2 \rfloor^{\frac{5}{4}} + k_2^{\frac{5}{3}} k_1^{\frac{5}{4}} \xi_1 \right\rfloor^{\frac{2}{5}},$$

$$G_2 = -C_1^{(2)} e_2 - W C_2^{(2)} e_3,$$

$$H = C_5^{(2)} \left[ \left[ \left( 1 - k_{I4} k_3^{\frac{5}{2}} k_2^{\frac{5}{3}} k_1^{\frac{5}{4}} \right) \xi_1 + \left( k_{I2} - k_{I4} k_3^{\frac{5}{2}} k_2^{\frac{5}{3}} \right) \lceil e_2 \rfloor^{\frac{5}{4}} + \left( k_{I3} - k_{I4} k_3^{\frac{5}{2}} \right) \lceil e_3 \rfloor^{\frac{5}{3}} + k_\xi \lceil e_5 \rfloor^5 \right]^0 + [-\overline{L}, \ \overline{L}] \right],$$

$$C_1^{(2)} = \gamma_2 \gamma_3 \left[ \gamma_1 \lceil \xi_1 \rfloor^{\frac{4}{5}} + \frac{m-4}{5} k_1^{\frac{m-4}{4}} \left( e_2 + k_1 \lceil \xi_1 \rfloor^{\frac{4}{5}} \right) \right] |\xi_1|^{\frac{m-9}{5}}$$
$$+ \gamma_3 \frac{m-3}{5} k_1^{\frac{5}{4}} k_2^{\frac{m-3}{3}} \left( e_3 + k_2 \left\lceil \lceil e_2 \rfloor^{\frac{5}{4}} + k_1^{\frac{5}{4}} \xi_1 \right\rfloor^{\frac{3}{5}} \right) \left| \lceil e_2 \rfloor^{\frac{5}{4}} + k_1^{\frac{5}{4}} \xi_1 \right|^{\frac{m-8}{5}},$$

$$C_2^{(2)} = \gamma_2 \gamma_3 \left( \lceil e_2 \rfloor^{\frac{m-4}{4}} + k_1^{\frac{m-4}{4}} \lceil \xi_1 \rfloor^{\frac{m-4}{5}} \right) + \gamma_3 \frac{m-3}{4} k_2^{\frac{m-3}{3}} \left( e_3 + k_2 \left\lceil \lceil e_2 \rfloor^{\frac{5}{4}} + k_1^{\frac{5}{4}} \xi_1 \right\rfloor^{\frac{3}{5}} \right) \left| \lceil e_2 \rfloor^{\frac{5}{4}} + k_1^{\frac{5}{4}} \xi_1 \right|^{\frac{m-8}{5}} |e_2|^{\frac{1}{4}},$$

$$C_3^{(2)} = \gamma_3 \left( \lceil e_3 \rfloor^{\frac{m-3}{3}} + k_2^{\frac{m-3}{3}} \left\lceil \lceil e_2 \rfloor^{\frac{5}{4}} + k_1^{\frac{5}{4}} \xi_1 \right\rfloor^{\frac{m-3}{5}} \right),$$

$$C_5^{(2)} = |e_5|^4 (\lceil e_5 \rfloor^{m-5} - 5k_\xi C_1^{(2)}).$$

Now we will show that $\mathcal{F}(\xi_1, \ e_2, \ e_3)$, which only depends on $(\xi_1, \ e_2, \ e_3)$ and not on $e_5$, can be designed to be positive definite by selection of the gains.

### B.2.1 Positive definitness of $\mathcal{F}(\xi_1, \ e_2, \ e_3)$

1. The first term in $\mathcal{F}$ is $k_3 C_3^{(2)} F_2$. We show that it is positive semidefinite. This is again a simple consequence of the fact that both continuous functions $C_3^{(2)}$ and $F_2$ vanish on the same set

$$S_2 = \left\{ (\xi_1, \ e_2, \ e_3) \in \mathbb{R}^3 | e_3 = -k_2 \left\lceil \lceil e_2 \rfloor^{\frac{5}{4}} + k_1^{\frac{5}{4}} \xi_1 \right\rfloor^{\frac{3}{5}} \right\},$$

and that they have the same sign.

2. Evaluating $\mathcal{F}$ on the set $S_2$, we obtain

$$\mathcal{F}|_{S_2} = k_2 W C_2^{(3)} F_3 + G_3 , \tag{B6}$$

where

$$F_3 = \left\lceil \lceil e_2 \rfloor^{\frac{5}{4}} + k_1^{\frac{5}{4}} \xi_1 \right\rfloor^{\frac{3}{5}},$$
$$G_3 = -C_1^{(3)} e_2 ,$$
$$C_1^{(3)} = \gamma_2 \gamma_3 \left[ \gamma_1 \lceil \xi_1 \rfloor^{\frac{4}{5}} + \frac{m-4}{5} k_1^{\frac{m-4}{4}} \left( e_2 + k_1 \lceil \xi_1 \rfloor^{\frac{4}{5}} \right) \right] |\xi_1|^{\frac{m-9}{5}},$$
$$C_2^{(3)} = \gamma_2 \gamma_3 \left( \lceil e_2 \rfloor^{\frac{m-4}{4}} + k_1^{\frac{m-4}{4}} \lceil \xi_1 \rfloor^{\frac{m-4}{5}} \right).$$

The first term in $\mathcal{F}|_{S_2}$ is $k_2 W C_2^{(3)} F_3$. It is positive semidefinite as a simple consequence of the fact that both continuous functions $C_2^{(3)}$ and $F_3$ vanish on the same set

$$S_3 = \left\{ (\xi_1, \ e_2) \in \mathbb{R}^2 | e_2 = -k_1 \lceil \xi_1 \rfloor^{\frac{4}{5}} \right\},$$

and that they have the same sign.

3. Evaluating $\mathcal{F}|_{S_2}$ on the set $S_3$ we obtain

$$\mathcal{F}|_{S_2 \cap S_3} = k_1 \gamma_1 \gamma_2 \gamma_3 |\xi_1|^{\frac{m-1}{5}} , \tag{B7}$$

which is positive for $k_1 > 0$, and vanishes only when $\xi_1 = 0$. Applying Lemma 1 to (B6) implies that $\mathcal{F}|_{S_2}$ can be rendered positive definite by selecting $k_2 > 0$ sufficiently large. Moreover, under the previous condition applying Lemma 1 to (B5) implies that $\mathcal{F}$ can be rendered positive definite by selecting $k_3 > 0$ sufficiently large.

### B.2.2 | Positive definiteness of $\mathcal{W}|_{S_1}$

In Equation (B4), the first term $\mathcal{F}$ is positive definite, and it vanishes on the set

$$S_4 = \{(\xi_1,\ e_2,\ e_3) \in \mathbb{R}^3 | \xi_1 = e_2 = e_3 = 0\} \ .$$

Evaluating $\mathcal{W}|_{S_1}$ on the set $S_4$, we obtain

$$\mathcal{W}|_{S_1 \cap S_4} = \tilde{k}_{I1} \lceil e_5 \rfloor^{m-1} [\lceil e_5 \rfloor^0 + [-\bar{L},\ \bar{L}]] \ .$$

$\mathcal{W}|_{S_1 \cap S_4}(e_5)$ is a multivalued function of the single variable $e_5$, since the term $[\lceil e_5 \rfloor^0 + [-\bar{L},\ \bar{L}]]$ is clearly a set. At $e_5 = 0$ the function $\mathcal{W}|_{S_1 \cap S_4}(0) = 0$. For $e_5 > 0$ the term $[\lceil e_5 \rfloor^0 + [-\bar{L},\ \bar{L}]] = 1 + [-\bar{L},\ \bar{L}]$ is an interval, that only contains positive numbers if $\bar{L} < 1$. Similarly, for $e_5 < 0$ the term $[\lceil e_5 \rfloor^0 + [-\bar{L},\ \bar{L}]] = -1 + [-\bar{L},\ \bar{L}]$ is an interval, that only contains negative numbers if $\bar{L} < 1$. From this we conclude that $\mathcal{W}|_{S_1 \cap S_4} > 0$ if $\bar{L} < 1$, that is, if $k_{I1} > L$. Under the previous conditions applying Lemma 2 to (B4) $\mathcal{W}|_{S_1} > 0$ for $\tilde{k}_{I1} > 0$ sufficiently small.

Finally, under the previous conditions and considering that according to (11) $\beta \geq b_m > 0$, applying Lemma 2 to (B3) $\mathcal{W} > 0$ for $k_4$ sufficiently large.

This concludes the proof of the fact that $\mathcal{W}(e) > 0$. The gains $k_1,\ k_2,\ k_3,\ k_4,\ \tilde{k}_{I1}$ to assure this fact can be calculated from the expressions (B7), (B6), (B5), (B3), (B4), respectively. In synthesis, the gain selection is as follows:

**Gain selection procedure**

(i) Choose any positive values for the parameters of the Lyapunov function $\gamma_1,\ \gamma_2,\ \gamma_3 > 0$.
(ii) Select $k_{I2}, k_{I3}, k_{I4}$ to be arbitrary positive, zero, or negative numbers.
(iii) Choose a value of $0 \leq \bar{L} < 1$. Select the gains successively as

$$
\begin{aligned}
&k_1 > 0 \ , \\[2mm]
&k_2 > \mathcal{K}_2(k_1) := \max_{|\xi_1|^{\frac{1}{5}} + |e_2|^{\frac{1}{4}} = 1} \frac{-G_3(\xi_1,\ e_2)}{WC_2^{(3)}(\xi_1,\ e_2)F_3(\xi_1,\ e_2)} \ , \\[2mm]
&k_3 > \mathcal{K}_3(k_1,\ k_2) := \max_{|\xi_1|^{\frac{1}{5}} + |e_2|^{\frac{1}{4}} + |e_3|^{\frac{1}{3}} = 1} \frac{-G_2(\xi_1,\ e_2,\ e_3)}{C_3^{(2)}(\xi_1,\ e_2,\ e_3)F_2(\xi_1,\ e_2,\ e_3)} \ , \\[2mm]
&\frac{1}{\tilde{k}_{I1}} > \mathcal{K}_{I1}(k_1,\ k_2,\ k_3,\ k_{I2},\ k_{I3},\ k_{I4},\ \bar{L}) := \max_{|\xi_1|^{\frac{1}{5}} + |e_2|^{\frac{1}{4}} + |e_3|^{\frac{1}{3}} + |e_5| = 1} \frac{-H(\xi_1,\ e_2,\ e_3,\ e_5)}{\mathcal{F}(\xi_1,\ e_2,\ e_3)} \ , \\[2mm]
&k_4 b_m > \mathcal{K}_4(k_1,\ k_2,\ k_3,\ k_{I2},\ k_{I3},\ k_{I4},\ \tilde{k}_{I1}) := \max_{|\xi_1|^{\frac{1}{5}} + |e_2|^{\frac{1}{4}} + |e_3|^{\frac{1}{3}} + |e_4|^{\frac{1}{2}} + |e_5| = 1} \frac{-G_1(e)}{C_4^{(1)}(e)F_1(e)} \ .
\end{aligned}
\tag{B8}
$$

Note that the functions to be maximized are all **r**-homogeneous of degree zero, and this implies that the maximum can be found on the unit sphere.

Be aware that the inequality $k_{I1} > L$ cannot be assured at this point, since $k_{I1}$ has to satisfy the fourth inequality. And so, $k_{I1} > L$ is more at this stage a restriction for $L$. However, we will be able to use any value of $L$ by utilizing a gain scaling below.

### B.3 | The effect of $\varphi_1(t,\ e)$

Now we regard the derivative of the LF in (B2), when only $\varphi_1(t,\ e)$ is considered, that is,

$$\dot{V}(e) = -\mathcal{W}(e) + \beta(t,\ e)C_4^{(1)}\varphi_1(t,\ e) \ .$$

Function $C_4^{(1)}$ is **r**-homogeneous of degree $m-2$, while $\mathcal{W}(e)$ is **r**-homogeneous of degree $m-1$. According to (11) $|\varphi_1(t,\ e)| \le L_1\|e\|_{\mathbf{r},\ p}$. Using (B3), we conclude that the previous inequality can be written as

$$\begin{aligned}\dot{\mathcal{V}}(e) &\le -(k_4\beta(t,\ e)C_4^{(1)}(e)F_1(e) + G_1(e)) + |\beta(t,\ e)||C_4^{(1)}||\varphi_1(t,\ e)| \\ &\le -\tilde{\mathcal{W}}(e) \\ \tilde{\mathcal{W}}(e) &:= k_4\beta(t,\ e)C_4^{(1)}(e)F_1(e) + G_1(e) - b_ML_1|C_4^{(1)}|\|e\|_{\mathbf{r},\ p}\ .\end{aligned}$$

As shown in the previous section, the first term in $\tilde{\mathcal{W}}(e)$ is non negative, and vanishes on the set $S_1$. Evaluating $\tilde{\mathcal{W}}(e)$ on this set, and using the fact that $C_4^{(1)}\big|_{S_1} = 0$, we obtain

$$\tilde{\mathcal{W}}\big|_{S_1} = G_1\big|_{S_1} > 0\ ,$$

which is positive, as shown in the previous section. Applying Lemma 2 to $\tilde{\mathcal{W}}(e)$ implies that it is possible to render $\tilde{\mathcal{W}}(e) > 0$ selecting $k_4$ sufficiently large. We conclude therefore that the closed-loop is GAS (finite-time stable) by selecting the gain $k_4$ large, for any value of $L_1$. The gains are obtained from the inequalities (B8), modifying the last inequality as

$$k_4b_m > \mathcal{K}_{4,\ p}(k_1,\ k_2,\ k_3,\ k_{I2},\ k_{I3},\ k_{I4},\ \overline{L},\ \tilde{k}_{I1},\ b_ML_1) := \max_{|\xi_1|^{\frac{1}{5}}+|e_2|^{\frac{1}{4}}+|e_3|^{\frac{1}{3}}+|e_4|^{\frac{1}{2}}+|e_5|=1} \frac{-G_1(e) + b_ML_1|C_4^{(1)}|\|e\|_{\mathbf{r},p}}{C_4^{(1)}(e)F_1(e)}\ . \tag{B9}$$

## B.4 The effect of $\psi(t,\ e_3)$

Adding the effect of the term $\psi(t,\ e_3)$ to the derivative of the LF, we obtain

$$\dot{\mathcal{V}}(e) \le -\tilde{\mathcal{W}}(e) + WC_2^{(1)}\psi(t,\ e_3)\ .$$

Function $C_2^{(1)}$ is **r**-homogeneous of degree $m-4$, while $\tilde{\mathcal{W}}(e)$ is **r**-homogeneous of degree $m-1$, and since it is positive definite there exist some $\alpha > 0$ such that $\tilde{\mathcal{W}}(e) \ge \alpha\|e\|_{\mathbf{r},\ p}^{m-1}$. According to (11) $|\psi(t,\ e_3)| \le L_0|e_3| \le L_0\|e\|_{\mathbf{r},\ p}^3$. We conclude that the previous inequality can be written as

$$\dot{\mathcal{V}}(e) \le -\tilde{\mathcal{W}}(e) + \delta WL_0\|e\|_{\mathbf{r},\ p}^{m-1} \le -(\alpha - \delta WL_0)\|e\|_{\mathbf{r},\ p}^{m-1}\ ,$$

so that $\dot{\mathcal{V}}(e)$ remains negative definite for some $L_0$ sufficiently small. In our concrete case, since according to (10) $\psi(t,\ e_3) = \sin(e_3 + r_3) - \sin(r_3) - e_3$, we have in the system (B1) that $\dot{e}_2 = W(e_3 + \psi(t,\ e_3)) = W(\sin(e_3 + r_3(t)) - \sin(r_3(t)))$, and the function $G_2$ in (B5) becomes $G_2 = -C_1^{(2)}e_2 - WC_2^{(2)}(\sin(e_3 + r_3(t)) - \sin(r_3(t)))$. And therefore Equation (B6) results in

$$\mathcal{F}\big|_{S_2} = k_2WC_2^{(3)}(\sin(F_3 + r_3(t)) - \sin(r_3(t))) + G_3\ .$$

It is not difficult to see that for large deviations of $F_3 + r_3(t)$ from zero, the required positivity of $C_2^{(3)}(\sin(F_3 + r_3(t)) - \sin(r_3(t)))$ is not satisfied. As it is well-known, the sinus function can be approximated by $\sin(x) \approx x$ for $x$ near to zero. And therefore, $\psi(t,\ e_3) = \sin(e_3 + r_3) - \sin(r_3) - e_3 \approx 0$ for small values of $e_3 + r_3$, and thus the condition is satisfied locally. This implies that the stability result obtained is only local.

## B.5 Gain scaling

Consider the closed-loop system given by (13), with $\lambda = 1$, which was used for the stability proof in the previous subsections. After the linear change of coordinates $\epsilon_i = \lambda e_i$, $i = 1, \ldots, 4$, and $z = \lambda\zeta$, with $\lambda > 0$, we arrive at the following dynamics

$$\begin{aligned}\dot{\epsilon}_1 &= \epsilon_2, \\ \dot{\epsilon}_2 &= W\epsilon_3 + W\lambda\psi\left(t,\ \frac{\epsilon_3}{\lambda}\right), \\ \dot{\epsilon}_3 &= \epsilon_4,\end{aligned}$$

$$\dot{e}_4 = \beta(t, e)\left[-k_4\lambda\left[k_3^{\frac{5}{2}}k_2^{\frac{5}{3}}k_1^{\frac{5}{4}}\frac{e_1}{\lambda} + k_3^{\frac{5}{2}}k_2^{\frac{5}{3}}\left\lceil\frac{e_2}{\lambda}\right\rfloor^{\frac{5}{4}} + k_3^{\frac{5}{2}}\left\lceil\frac{e_3}{\lambda}\right\rfloor^{\frac{5}{3}} + \left\lceil\frac{e_4}{\lambda}\right\rfloor^{\frac{5}{2}}\right]^{\frac{1}{5}} + z + \lambda\varphi(t, e)\right]$$

$$= \beta(t, e)\left[-k_4\lambda^{\frac{1}{2}}\left[\left(\lambda^{\frac{1}{3}}k_3\right)^{\frac{5}{2}}\left(\lambda^{\frac{1}{4}}k_2\right)^{\frac{5}{3}}\left(\lambda^{\frac{1}{5}}k_1\right)^{\frac{5}{4}}e_1 + \left(\lambda^{\frac{1}{3}}k_3\right)^{\frac{5}{2}}\left(\lambda^{\frac{1}{4}}k_2\right)^{\frac{5}{3}}\lceil e_2\rfloor^{\frac{5}{4}} + \left(\lambda^{\frac{1}{3}}k_3\right)^{\frac{5}{2}}\lceil e_3\rfloor^{\frac{5}{3}} + \lceil e_4\rfloor^{\frac{5}{2}}\right]^{\frac{1}{5}}\right.$$

$$+z + \lambda\varphi(t, e)]$$

$$\dot{z} = -k_{I1}\lambda\left[\frac{e_1}{\lambda} + k_{I2}\left\lceil\frac{e_2}{\lambda}\right\rfloor^{\frac{5}{4}} + k_{I3}\left\lceil\frac{e_3}{\lambda}\right\rfloor^{\frac{5}{3}} + k_{I4}\left\lceil\frac{e_4}{\lambda}\right\rfloor^{\frac{5}{2}}\right]^0$$

$$= -k_{I1}\lambda\left[e_1 + \lambda^{-\frac{1}{4}}k_{I2}\lceil e_2\rfloor^{\frac{5}{4}} + \lambda^{-\frac{2}{3}}k_{I3}\lceil e_3\rfloor^{\frac{5}{3}} + \lambda^{-\frac{3}{2}}k_{I4}\lceil e_4\rfloor^{\frac{5}{2}}\right]^0.$$

Note that this dynamics is identical to the original one if we perform the following changes (scalings):

$$k_1 \to \lambda^{\frac{1}{5}}k_1, \quad k_2 \to \lambda^{\frac{1}{4}}k_2, \quad k_3 \to \lambda^{\frac{1}{3}}k_3, \quad k_4 \to \lambda^{\frac{1}{2}}k_4, \quad \varphi \to \lambda\varphi,$$

$$k_{I1} \to \lambda k_{I1}, \quad k_{I2} \to \lambda^{-\frac{1}{4}}k_{I2}, \quad k_{I3} \to \lambda^{-\frac{2}{3}}k_{I3}, \quad k_{I4} \to \lambda^{-\frac{3}{2}}k_{I4}.$$

Since the two systems are related by a linear change of coordinates, this implies that they have the same stability properties, also they are both finite-time stable (if one is).